**Climate
of the Past**
Open Access
Discussions

Multi-proxy fingerprint of Heinrich event 4 in Greenland ice core records

M. Guillevic[1,2], L. Bazin[1], A. Landais[1], C. Stowasser[2], V. Masson-Delmotte[1], T. Blunier[2], F. Eynaud[3], S. Falourd[1], E. Michel[1], B. Minster[1], T. Popp[2], F. Prié[1], and B. M. Vinther[2]

[1]Laboratoire des Sciences du Climat et de l'environnement, UMR CEA/CNRS/UVSQ 8212, Gif-sur-Yvette, France
[2]Centre for Ice and Climate, Niels Bohr Institute, University of Copenhagen, Copenhagen, Denmark
[3]Laboratoire EPOC, UMR CNRS 5805 EPOC-OASU, Université Bordeaux 1, Talence, France

CPD

10, 1179–1222, 2014

Heinrich event 4 in Greenland ice core records

M. Guillevic et al.

Title Page

Abstract | Introduction

Conclusions | References

Tables | Figures

|◄ | ►|

◄ | ►

Back | Close

Full Screen / Esc

Printer-friendly Version

Interactive Discussion

Abstract

Glacial climate was characterised by two types of abrupt events. Greenland ice cores record Dansgaard–Oeschger events, marked by abrupt warming in-between cold, stadial phases. Six of these stadials coincide with major Heinrich events (HE), identified from ice-rafted debris (IRD) and large excursions in carbon and oxygen stable isotopic ratios in North Atlantic deep sea sediments, documenting major ice sheet collapse events. This finding has led to the paradigm that glacial cold events are induced by the response of the Atlantic Meridional Overturning Circulation to such massive freshwater inputs, supported by sensitivity studies conducted with climate models of various complexities. This mechanism could however never be confirmed or infirmed because the exact timing of Heinrich events and associated low latitude hydrological cycle changes with respect to Greenland stadials has so far remained elusive. Here, we provide the first multi-proxy fingerprint of H4 within Stadial 9 in Greenland ice cores through ice and air proxies of low latitude climate and water cycle changes. Our new dataset demonstrates that Stadial 9 consists of three phases, characterised first by Greenland cooling during 550 ± 60 years (as shown by markers of Greenland temperature δ^{18}O and δ^{15}N), followed by the fingerprint of Heinrich Event 4 as identified from several proxy records (abrupt decrease in ^{17}O excess and Greenland methane sulfonic acid (MSA), increase in CO_2 and methane mixing ratio, heavier δD–CH_4 and $\delta^{18}O_{atm}$), lasting 740 ± 60 years, itself ending approximately 390 ± 50 years prior to abrupt Greenland warming. Preliminary investigations on GS-13 encompassing H5, based on the ice core proxies δ^{18}O, MSA, $\delta^{18}O_{atm}$, CH_4 and CO_2 data also reveal a 3 phase structure, as well as the same sequence of events. The decoupling between stable cold Greenland temperature and low latitude HE imprints provides new targets for benchmarking climate model simulations and testing mechanisms associated with millennial variability.

1   Introduction

Glacial climate is characterised by millennial variability, recorded with specific expressions in different archives and at different latitudes (Voelker, 2002; Clement and Peterson, 2008). Greenland ice core records of ice δ^{18}O, a qualitative proxy of air temperature, have unveiled at high resolution the succession of cold phases (Greenland Stadials, GS) and warm phases (Greenland Interstadials, GI) forming the 25 Dansgaard–Oeschger events (DO) of the last glacial period (NGRIP members, 2004). DO events are recorded through climatic and environmental changes in other North Atlantic/European archives such as speleothems (Genty et al., 2010; Boch et al., 2011), pollen and marine bioindicators from North Atlantic marine cores (e.g. Voelker, 2002; Sánchez Goñi and Harrison, 2010), with interstadials being characterised in Western Europe by warmer and more humid conditions while stadials are associated with a dry and cold climate. The tropics also exhibit a fingerprint of DO events as suggested e.g. by (i) variations in monsoon strength (e.g. recorded in speleothem growth rate and calcite δ^{18}O, Wang et al., 2001), (ii) changes in the atmospheric methane concentration (as measured in ice cores, Chappellaz et al., 1993, 2013) with its main source located at low latitudes during glacial periods (e.g. Baumgartner et al., 2012), or (iii) changes in the isotopic composition of atmospheric oxygen δ^{18}O$_{atm}$ (measured in air from ice cores, Landais et al., 2007; Severinghaus et al., 2009), reflecting at this time scale changes in the low latitude water cycle and global biosphere productivity (Bender et al., 1994b). Such variations in the low latitude climate are probably due to shifts in the Intertropical Convergence Zone (ITCZ, e.g. Peterson et al., 2000). The bipolar seesaw identified between each Greenland DO event and its Antarctic counterpart (EPICA community members, 2006; Capron et al., 2010) supports a key role of reorganisations of the Atlantic Ocean inter-hemispheric heat transport (Stocker and Johnsen, 2003), likely associated with strong variations of the Atlantic Meridional Oceanic Circulation (AMOC) intensity.

In addition to palaeoclimate records showing this DO succession, a prominent feature identified in North Atlantic deep cores is the occurrence of ice-rafted debris (IRD, Ruddiman, 1977). These IRD are interpreted as the signature of massive iceberg discharges in the North Atlantic Ocean originating from the Laurentide, Icelandic, British–Irish and Fennoscandian ice sheets (e.g., Heinrich, 1988; Bond et al., 1993). Six such Heinrich events (HE, numbered H1 to H6, Fig. 1) have been unambiguously identified during GS phases of the last glacial period (e.g., Bond et al., 1992; Hemming, 2004). Minor events identified in one or a few cores have additionally been reported (H5a (Rashid et al., 2003), H7a, H7b, H8 to H10 (Rasmussen et al., 2003), Fig. 1). In addition to the IRD layers, periods of low surface salinity likely due to enhanced fresh-water fluxes have been evidenced in a deep core from the Celtic margin (Fig. 1 blue areas, Eynaud et al., 2012). Studies on the composition of each IRD layer have demonstrated the dominant Laurentide origin of H2, H4 and H5, while H3 and H6 are mainly due to icebergs delivery from European ice sheets (Grousset et al., 1993, 2000; Gwiazda et al., 1996; Hemming et al., 1998; Snoeckx et al., 1999; Jullien et al., 2006). H1 results from the collapse of several ice sheets (Stanford et al., 2011).

The coincidence of HEs and stadials have led to the paradigm that Greenland stadial/interstadial variability is related to freshwater-induced changes in AMOC. Indeed, the response of climate models of different complexities to freshwater perturbations bears similarities with palaeoclimate observations (e.g., Kageyama et al., 2013). However, several lines of evidence suggest that HE are shorter than the corresponding GS (Peters et al., 2008; Roche et al., 2004) and occur after the AMOC entered a weakening trend (Flückiger et al., 2006; Marcott et al., 2011). Unfortunately, uncertainties associated with marine and ice core chronologies have so far prevented the determination of the exact timing of Heinrich events with respect to GS (Sánchez Goñi and Harrison, 2010; Austin and Hibbert, 2012). Therefore the mechanisms relating iceberg discharge, low latitude climate change and Greenland temperature change during stadials remain debated (Hemming, 2004; Clement and Peterson, 2008; Mulitza et al., 2008).

Heinrich event 4 in Greenland ice core records

M. Guillevic et al.

North Atlantic marine cores are the only archive to register Heinrich events *stricto senso* (i.e. the IRD layer) together with their impact on ocean circulation characteristics. They usually contain a sufficient amount of organic material to allow ^{14}C dating. However, a large uncertainty of this method is the estimation of the reservoir age, that varies from ~ 400 a at present up to $\sim 1900 \pm 700$ a at the end of H1 in the North Atlantic (e.g. Waelbroeck et al., 2001; Bondevik et al., 2006; Stern and Lisiecki, 2013). The reservoir age is likely modified during Heinrich events because of North Atlantic Deep Water (NADW) circulation slow down/shut down and continental water release by iceberg discharges (Hemming, 2004; Ritz et al., 2008). Additionally, HE cause abrupt changes in sedimentation rates, further challenging dating the onset and duration of these events.

The impact of Heinrich events is not limited to the North Atlantic but has a signature in mid to low latitude proxies. For instance speleothem growth rate and calcite isotopes (Kanner et al., 2012; Wang et al., 2007; Mosblech et al., 2012) indicate a southwards displacement of the intertropical convergence zone (ITCZ) which is more pronounced during stadials associated with Heinrich events than during stadials without Heinrich event. Model simulations indeed produce in a few years a southwards displacement of the ITCZ over the Atlantic Ocean and its margins in response to North Atlantic cooling (e.g. Chiang et al., 2008; Cvijanovic and Chiang, 2013). Speleothems from low latitudes have the advantage to provide the best absolute chronology amongst palaeo archives so far, through uranium-thorium dating of the calcite. Associated uncertainties can be as low as $\sim \pm 1\%$ (2σ) of the absolute age for the Hulu cave record (Wang et al., 2001). In practice, the accuracy of speleothem chronologies can decrease due to e.g. possible hiatus, varying growth rate in-between U-Th time points, presence of a variable "initial" [230]Th in the calcite (e.g., Fleitmann et al., 2008). Severinghaus et al. (2009) proposed that calcite $\delta^{18}O$ from South-East Asia speleothems and $\delta^{18}O_{atm}$ variations registered in the air entrapped from ice cores are both mostly controlled by latitudinal shifts of the ITCZ and associated changes in the isotopic composition of tropical precipitation. This common driving climatic mechanism therefore offers a direct link between

Heinrich event 4 in Greenland ice core records

M. Guillevic et al.

Printer-friendly Version

Interactive Discussion

speleothem and ice core archives. However, climate-independent markers have not yet been identified that would allow to synchronise speleothems to other archives from different latitudes such as marine cores, preventing a precise comparison of the timing of events between high, mid and low latitudes associated with Heinrich events.

5 In Greenland ice cores, DO events are well dated thanks to annual layer counting. For the GICC05 timescale used here, absolute ages are estimated with $\sim 3\%$ uncertainty (2σ) during the glacial period (Svensson et al., 2008, and Appendix A1). A precise synchronisation between marine and ice cores during HE remains however difficult to establish due to the lack of a HE fingerprint within the Greenland ice core
10 records. Neither ice $\delta^{18}O$ (a qualitative proxy of temperature) nor Greenland temperature (reconstructed from $\delta^{15}N$ measurements in the air bubbles based on firn gas gravitational and thermal fractionation) do exhibit any specific fingerprint of HEs during the corresponding stadials (Figs. 1 and 4 and e.g., Kindler et al., 2014). However, Greenland ice cores do provide proxy records sensitive to high, mid and low latitude
15 climate changes. This archive therefore gives the opportunity to explore time leads and lags in between events happening at different latitudes. Indeed, precious information on the sequence of events between mid and high latitude climate arises from the combination of all stable water isotopologues in Greenland ice cores. $\delta^{18}O$ is a qualitative proxy of local Greenland temperature showing the well-known GS-GI pattern.
20 Deuterium excess ($d - \mathrm{excess} = \delta D - 8 \times \delta^{18}O$, Dansgaard, 1964) is influenced by the vapour source temperature and relative humidity, as well as the condensation temperature of precipitation (Masson-Delmotte et al., 2005). By construction, the definition of ^{17}O excess ($^{17}O\,\mathrm{excess} = \ln(\delta^{17}O + 1) - 0.528\ln(\delta^{18}O + 1)$) makes this parameter less sensitive than d-excess to the vapour distillation history, hence to local temperature
25 (Masson-Delmotte et al., 2005; Landais et al., 2012). It therefore better reflects the climatic conditions during evaporation or moisture recharge of Greenland vapour source, in particular the relative humidity that controls kinetic fractionation during such processes.

M. Guillevic et al.

In this study, we investigate multiple climate proxies registered in Greenland ice cores (NEEM (North Greenland Eemian Ice Drilling), NGRIP (North Greenland Ice Core Project) and GISP2 (Greenland Ice Sheet Project 2), map Fig. 2) on the same chronology (GICC05 (Greenland Ice Core Chronology 2005), Appendix A), giving information about the local as well as the remote climate on exactly the same timescale. The aim is to reconstruct the sequence of events surrounding Heinrich events at low and high latitudes. We focus on GS-9, 38 220–39 900 a b2k (years before AD 2000 on the GICC05 timescale), between GI-8 and GI-9, characterised by the occurrence of the major H4 IRD event of mostly Laurentide ice sheet (LIS) origin (Hemming, 2004; Jullien et al., 2006). This event occurs during Marine Isotope Stage 3, a period consisting of short-lived and frequent DO events (NGRIP members, 2004). In the following we will argue that the climatic fingerprint of H4 can be identified in multiple proxy records sensitive to climate and environmental changes at high, mid and low latitudes, archived in the ice and air of Greenland ice cores.

2 Measurement method

2.1 ^{17}O excess

We have performed on the NEEM ice core (Dahl-Jensen and NEEM community members, 2013, localisation on Fig. 2) the first measurements of ^{17}O excess, spanning a sequence of 3 DO events and encompassing GS-9. The method for ^{17}O excess measurements was first described in Luz and Barkan (2005). 2 microlitres of water are fluorinated under a helium flow and the resulting oxygen O_2 is purified on a molecular sieve before being trapped in a manifold immersed in liquid helium. O_2 is then measured on a DELTA V isotope ratio mass spectrometer vs. pure oxygen. Dual inlet measurements last 75 min for each converted oxygen sample. Each water sample has been converted and measured at least twice. Every day, we use 2 homemade water standards in our

fluorination line to check the stability of the measurements and to perform calibrations. The resulting pooled standard deviation for ^{17}O excess measurements is 5 permeg.

For this study with δ^{18}O varying between −43 and −38‰, we have mainly used 3 homemade standards at around −32, −40 and −58‰. These homemade standards are calibrated vs. V-SMOW (Vienna Standard Mean Ocean Water, δ^{18}O = 0‰; ^{17}O excess = 0 permeg) and SLAP (Standard Light Antarctic Precipitation, δ^{18}O = −55.5‰; ^{17}O excess = 0 permeg, Luz et al., 2009; Schoenemann et al., 2013). The calibration of our raw ^{17}O excess data can then be performed in two different ways. In a first attempt, we have simply subtracted from all raw ^{17}O excess data the ^{17}O excess difference between the measured and the calibrated standard at −40‰. In a second attempt, we have used a 2 points calibration between measured and accepted values of V-SMOW and SLAP so that the ^{17}O excess correction increases with the δ^{18}O difference between O$_2$ obtained from the sample conversion and O$_2$ obtained from V-SMOW conversion. We show in Fig. 3b the comparison of ^{17}O excess evolution after these two corrections as well as the raw data. The general evolution of the ^{17}O excess profile and the particular separation in phases over GS-9 is not affected by the different corrections.

Finally, note that the measurements were done in two rounds, with a first series measured in spring 2011 and a second one at the beginning of 2012. Comparisons of the profiles are displayed in Fig. 3a after correction with the two points (V-SMOW vs. SLAP) calibration. Note that for samples before 39.5 ka, the measurements were not necessary performed over the same exact depth levels, which makes the intercomparison less accurate. Both the mean levels and the variability are very coherent between the two ^{17}O excess profiles.

2.2 δ^{18}O$_{atm}$

Our new δ^{18}O$_{atm}$ (δ^{18}O of O$_2$) dataset measured on the NEEM ice core consists of 95 data points with replicates. A melt-refreeze technique has been used to extract the air from the ice samples. Our isotope ratio mass spectrometer is equipped with 10

Faraday cups to measure simultaneously the isotopic ratios $\delta^{18}O$ and $\delta^{15}N$ as well as the elemental ratios O_2/N_2 and CO_2/N_2 (Landais et al., 2010).

To reconstruct the past $\delta^{18}O_{atm}$ signal, $\delta^{18}O$ measurements have been first corrected for eventual gas loss during ice storage using the $\delta O_2/N_2$ ratio measured in the same samples (Landais et al., 2010):

$$\delta^{18}O_{\text{gas loss corrected}} = \delta^{18}O_{\text{measured}} + 0.01\,(\delta O_2/N_2 + 10) \tag{1}$$

The obtained data are then corrected for thermal and gravitational fractionation occurring in the firn, using the $\delta^{15}N_{therm}$ (thermal fractionation of nitrogen isotope) and $\delta^{15}N_{grav}$ (gravitational fractionation of nitrogen isotope) scenarios reconstructed using the measured $\delta^{15}N$ data and firn modelling (Guillevic et al., 2013; Landais et al., 2010, and references therein):

$$\delta^{18}O_{atm} = \delta^{18}O_{\text{gas loss corrected}} - 1.6\,\delta^{15}N_{therm} - 2\,\delta^{15}N_{grav} \tag{2}$$

The resulting $\delta^{18}O_{atm}$ pooled standard deviation is 0.03 ‰ (Landais et al., 2010). The $\delta^{18}O_{atm}$ dataset is reported on the GICC05 timescale (Fig. 4g) using the NEEM gas age scale from Guillevic et al. (2013). The obtained profile is in agreement with previously published results from Severinghaus et al. (2009) measured on the Siple Dome ice core, Antarctica (Appendix A2, Fig. 9). The advantage of using the NEEM rather than the Siple Dome $\delta^{18}O_{atm}$ data reside in the smaller NEEM ice-gas synchronisation uncertainty during GS-9 (Appendix A2).

3 Results and discussion

3.1 ^{17}O excess record

Two major features can be identified in the ^{17}O excess record covering DO-7 to DO-10 (Fig. 4d): (i) high ^{17}O excess levels correspond to GI and low levels to GS, with the exception of a persistent high plateau during GI-10, GS-10 and GI-9; (ii) the ^{17}O excess

Heinrich event 4 in
Greenland ice core
records

M. Guillevic et al.

increase from GS to GI is gradual and starts up to several centuries before the GI onset seen in the δ^{18}O record. We observe the largest decoupling between δ^{18}O and ^{17}O excess during GS-9, ^{17}O excess decreasing after the δ^{18}O decrease at the beginning of GS-9 and increasing several centuries before the δ^{18}O increase at the beginning of GI-8.

The low ^{17}O excess levels could be due to a higher relative humidity during vapour formation and/or more recharge of the vapour on the way to Greenland, causing a decrease in ^{17}O excess (e.g., Risi et al., 2010). A preponderance of summer precipitation in Greenland during stadials (when relative humidity is highest in the source regions) compared to winter precipitation may also lower the ^{17}O excess. These scenarios are in agreement with a southwards shift of the vapour source during stadials as already suggested by the high d-excess values (Johnsen et al., 1989; Masson-Delmotte et al., 2005; Jouzel et al., 2007).

3.2 Multi-proxy identification of a 3-phase sequence during GS-9

Within GS-9 of constantly low δ^{18}O and high d-excess values, three distinct phases are inferred from ^{17}O excess variations (Fig. 4d, Table 1): phase 1 (39 900–39 350 a b2k), corresponding to the beginning of GS-9, is marked by high ^{17}O excess values (mean = 56 permeg); phase 2 (39 350–38 610 a b2k) corresponds to low ^{17}O excess values (down to 34 permeg); finally during phase 3 (38 610–38 220 a b2k) ^{17}O excess reaches high interstadial levels again (mean = 57 permeg). The cold and stable Greenland temperature during the entire GS-9 is further confirmed by an independent temperature reconstruction based on firn gas fractionation (δ^{15}N, Fig. 4b and Guillevic et al., 2013). Our new data therefore suggest a decoupling between stable, cold Greenland temperatures and changes in the climate of the mid latitude source region for Greenland precipitation. From phase 1 to phase 2, the lower ^{17}O excess but constant d-excess signals could be due to a southwards shift of the moisture source, leading to more recycling of the vapour on the way to Greenland without necessary source temperature changes (Fig. 4c and d).

Using our new high resolution $\delta^{18}O_{atm}$ measurements of air entrapped in the NEEM ice core over the same sequence of events, we are able to evidence a global signature for this three phase sequence of GS-9 at mid latitudes. Indeed, earlier studies have shown that millennial $\delta^{18}O_{atm}$ variations are global responses to water cycle changes in the northern tropics (Severinghaus et al., 2009; Landais et al., 2010), where ITCZ shifts drive changes in precipitation isotopic composition (Lewis et al., 2010; Pausata et al., 2011). Our 95 new measurements of $\delta^{18}O_{atm}$ depict a stable, low $\delta^{18}O_{atm}$ during phase 1, followed by an increase over phase 2 (+0.14‰), and finally a stable high plateau during phase 3 (Fig. 4g). The onsets of changes of $\delta^{18}O_{atm}$ and ^{17}O excess occur synchronously at the beginning of phase 2 (ice-gas synchronisation uncertainty less than ±100 a, Appendix A2), but the increase of $\delta^{18}O_{atm}$ is much slower than the observed changes in ^{17}O excess; this is expected because of the long residence time of oxygen in the atmosphere (1000–2000 a, Bender et al., 1994a; Hoffmann et al., 2004).

Additionally, MSA (methane sulfonic acid) and methane from ice cores also support the same three phase structure during GS-9. First, recent works suggest that MSA from Arctic ice cores could be used as a proxy for sea-ice extent (Abram et al., 2013; O'Dwyer et al., 2000; Sharma et al., 2012). If so, the high resolution MSA data from the GISP2 Greenland ice core (Fig. 4e and Saltzman et al., 1997) suggests that the onset of phase 2 is marked by a large sea-ice expansion in the North Atlantic. Such a sea-ice expansion is likely associated with a southwards shift of storm tracks and, hence, Greenland moisture sources, as already suggested by the low ^{17}O excess level. Southward shifts of ITCZ simulated in response to North Atlantic cooling and increased sea ice cover (Chiang et al., 2008) could also explain the simultaneous $\delta^{18}O_{atm}$ signal.

Second, in the gas phase, the global expression of the three phase sequence is imprinted in the records of CH_4 and its hydrogen isotopic composition ($\delta D–CH_4$) (Fig. 4h and f, respectively). Phase 1 is characterised by a minimum in methane mixing ratio, whereas the onset of phase 2 is marked by a 20 ppb abrupt increase (Fig. 4h and Chappellaz et al., 2013) accompanied by a 8 ± 4.8‰ increase in $\delta D–CH_4$ (Bock et al., 2010). Such a shift would be in agreement with clathrate release, but is not supported

Heinrich event 4 in Greenland ice core records

M. Guillevic et al.

Title Page

Abstract | Introduction

Conclusions | References

Tables | Figures

|◄ | ►|

◄ | ►

Back | Close

Full Screen / Esc

Printer-friendly Version

Interactive Discussion

by the following stable plateau of methane mixing ratio throughout phase 2 and 3. We rather favour a source mix change or/and heavier isotopic composition of tropical precipitation (Möller et al., 2013) at the onset of phase 2. The mixing ratio increase is consistent with the activation of new methane sources, in e.g. South America as simulated by Hopcroft et al. (2011), associated with a southward ITCZ shift at the onset of phase 2. Moreover, such southward ITCZ shift is expected to produce more depleted precipitation in the SH (Southern Hemisphere) tropics and heavier precipitation in the NH (Northern Hemisphere) tropics (Pausata et al., 2011; Lewis et al., 2010). The increase in both $\delta D-CH_4$ and $\delta^{18}O_{atm}$ at the onset of phase 2 are consistent with this mechanism, provided that NH tropics remain the main source of methane and oxygen. A minor part of the $\delta D-CH_4$ increase can be due to oxidation of methane in the troposphere, consuming preferentially the light methane isotopologues, if the mean atmospheric temperature decreases at the onset of phase 2 (Lewis et al., 2010; Bock et al., 2010; Sowers, 2006).

Finally, two abrupt ~ 20 ppm increases in the atmospheric CO_2 concentration recently unveiled from high resolution Antarctic ice core records occur at the onsets of phase 2 and phase 3 (Fig. 4i and Ahn et al., 2012). After Antarctic and Greenland gas record synchronisation through CH_4 (Appendix A2), our study evidences that the CO_2 rise at the onset of phase 2 is synchronous (± 100 a) with cooling of the North Atlantic and southwards shift of the ITCZ, as suggested by the other NEEM ice core proxy variations. Different mechanisms are proposed to explain this CO_2 rise, as already discussed in Ahn et al. (2012): most probably upwelling in the Southern Ocean around Antarctica as suggested by increased opal burial rates in marine cores (Anderson et al., 2009), with a potential minor contribution from upwelling off the NW African coast (Jullien et al., 2007; Itambi et al., 2009; Mulitza et al., 2008). The causes of such modifications of the oceanic carbon storage may involve strengthening and/or southwards shift of the SH westerlies, and/or AMOC slow down, and therefore remain debated (e.g., Toggweiler et al., 2006; Völker and Köhler, 2013; Menviel et al., 2014).

Title Page

Abstract | Introduction

Conclusions | References

Tables | Figures

|◄ | ►|

◄ | ►

Back | Close

Full Screen / Esc

Printer-friendly Version

Interactive Discussion

The proposed sequence of events is summarised in Fig. 5. Altogether, our multi-proxy ice core dataset reveals a 740 a long period starting 550 a after the onset of GS-9 (phase 2) which is marked by North Atlantic sea ice expansion and southward shifts in North Atlantic storm tracks and ITCZ. Based on the discussed proxies, we therefore propose that H4 takes place in phase 2. The transition to phase 3 is characterised by reversed variations, with ^{17}O excess, MSA and δD−CH$_4$ reaching interstadial values 200 to 400 a prior to the increase in δ^{18}O marking the onset of GI-8. We explain this pattern by a gradual northward shift of the ITCZ and of the sea-ice cover, associated with lighter precipitation in the NH tropics and heavier precipitation in the SH tropics. The flat methane and δ^{18}O$_{atm}$ records suggest globally stable methane budget and biosphere productivity, possibly due to compensating effects at different latitudes.

3.3 Comparison with marine core records from the North Atlantic

The three phase sequence identified in low to mid latitude proxies in Greenland ice cores during GS-9 is also found in low to mid latitude climate archives. Indeed, combining North Atlantic marine cores from different latitudes along the European margin (Figs. 2 and 6 and also Naughton et al., 2009), Stadial 9 can again be subdivided into 3 phases: (i) prior to the Laurentide IRD delivery, cold conditions are already depicted in the eastern part of the so-called Ruddiman belt (Ruddiman, 1977), at 45–55° N (e.g. Fig. 6a, core MD95–2006, Peters et al., 2008; Dickson et al., 2008) while interstadial conditions persist around the Iberian Peninsula at 35–42° N (e.g. Fig. 6d, core MD95-2040, de Abreu et al., 2003); (ii) the onset of the Laurentide IRD delivery coincides with a possible further cooling at high latitudes, while Iberia enters into cold stadial conditions; (iii) once low Laurentide IRD levels are registered again, mild to interstadial conditions are recorded around the Iberian Peninsula, while cold temperatures persist at 45–55° N. In-between 40 and 57° N, cores MD04-2845 and MD95-2002 suggest that the situation might be intermediate, with a slight lag of the Laurentide IRD layer behind the polar species *Neogloboquadrina pachyderma* sinistral increase (Fig. 6b, c). Higher resolution data as well as climate-independent synchronisation tools in between

marine cores (such as measurments to detect specific palaeomagnetic events and/or volcanic ash layers) are necessary for a better description.

We previously argued for a southward shift of the ITCZ at the onset of phase 2 of our Greenland ice core sequence, with fingerprints in CH_4, $\delta D-CH_4$, ^{17}O excess and $\delta^{18}O_{atm}$. Bringing together marine and ice core records, we suggest that this ITCZ shift coincides with the onset of colder conditions in the Iberian Peninsula and also corresponds to the purge of the LIS, i.e. the beginning of H4. With this assumption, the inferred start of H4 would be $39\,350 \pm 1520$ a b2k on the GICC05 chronology. This iceberg discharge would lead to North Atlantic cooling, southward expansion of North Atlantic sea-ice cover and southward ITCZ shift, as simulated by climate models (Chiang et al., 2008). Within phase 2, the secondary minima in ^{17}O excess data at $\sim 38\,700$ a b2k (blue arrows, Fig. 4) could reflect another massive iceberg delivery. Interestingly, such fine structure is consistent with a couple of marine cores with high resolution data that register the H4 IRD layer as 2 distinct sub-events (in particular MD95-2002 and MD95-2006, Fig. 6).

Finally, during phase 3, we note a progressive shift towards interstadial conditions first indicated by low to mid latitudes ice core proxies (Fig. 4, $\delta D-CH_4$, ^{17}O excess, MSA). The ^{17}O excess (and possibly $\delta D-CH_4$) shifts precede the MSA increase; this would be consistent with a progressive northwards progression of the climate recovery towards interstadial climate conditions. This is in agreement with marine cores from low to mid latitudes suggesting the start of a progressive AMOC recovery before full interstadial climate conditions are reached (e.g., Vautravers et al., 2004). The combination of ice and marine core data therefore supports the following sequence of events: end of the iceberg delivery in the North Atlantic, northwards shift of the ITCZ and progressive AMOC restart, followed by a gradual marginal sea-ice cover retreat and finally the abrupt Greenland warming (Fig. 5).

3.4 Heinrich event 5: a similar sequence of events compared to H4

The Heinrich event 5 IRD layer is mainly originating from the LIS (Hemming, 2004) and can be found in marine cores during Stadial 13. Figure 7 compiles published ice core data of interest covering GS-13: NEEM δ^{18}O, GISP2 MSA, NGRIP δ^{18}O$_{atm}$, NEEM CH$_4$, together with TALDICE (Talos Dome, Antarctica) CH$_4$ and CO$_2$ data. The NEEM δ^{18}O data, in agreement with other Greenland ice cores as well as Greenland d-excess data (Masson-Delmotte et al., 2005; Jouzel et al., 2007), show a stable GS-13. The GISP2 MSA concentration data (Saltzman et al., 1997) show the same pattern of changes as during GS-9, marked by 3 phases. Phase 1 starts with the δ^{18}O decrease at the onset of GS-13 and ends by the MSA drop at 48 200 a b2k ±1980 a (140±40 a after the onset of GS-13). The onset of phase 2 is accompanied by abrupt increases in the atmospheric concentration of methane (+40 ppb in NEEM, +45 ppb in TALDICE) and possibly CO$_2$ (+5 ppm in TALDICE, less clear in the Byrd CO$_2$ record, Chappellaz et al., 2013; Bereiter et al., 2012; Ahn et al., 2012), as well as a gradual increase in the NGRIP δ^{18}O$_{atm}$ (Huber et al., 2006). Phase 2 as defined by the low MSA level lasts 860 ± 60 a (∼ 120 a longer than phase 2 of GS-9). Phase 3 starts by the increase in MSA prior to GI-12 and has an overall duration of 480 ± 50 a, comparable to the duration of phase 3 of GS-9.

This brief inspection of GS-13 confirms the substructure of 3 phases, the sequence of events and the durations observed for GS-9. If the same mechanisms are at play, we expect the following signals: a high [17]O excess during phases 1 and 3 and a low plateau during phase 2, and a high δD−CH$_4$ during phase 2 compared to lower δD−CH$_4$ during phases 1 and 3.

3.5 Constraints on the duration of iceberg delivery

Our proposed duration of the Heinrich event climate imprint (phase 2) may help to constrain the duration of the iceberg delivery itself, even though both are strictly speaking not the same. First, the sharp increase in Laurentide IRD in marine cores from the

North Atlantic and the clear onset of phase 2 as seen in various ice core proxies favour a synchronous onset of H4 and phase 2. Then, concerning the duration of the iceberg delivery, we propose the following scenarios:

– if the climate recovery at mid to low latitudes (onset of phase 3) is delayed after the end of the iceberg pulse, as suggested by transient model simulations (by ∼ 200 a, e.g. Roche et al., 2010; Otto-Bliesner and Brady, 2010), we propose that phase 2 (740 ± 60 a for H4, 860 ± 60 a for H5) may be a maximum iceberg delivery duration;

– if the climate recovery and the end of the IRD layer are synchronous as observed in e.g. marine core MD95-2040 at 40° N (Fig. 6), then the duration of phase 2 is the best estimate for the iceberg delivery duration;

– if a low amount of icebergs still brings IRD but has no climatic effect and/or does not reach the European margin, and considering that most North Atlantic marine cores do not record Laurentide IRD once full interstadial climate conditions are back (e.g., Hemming, 2004), we propose a maximum IRD delivery duration of phase 2 + phase 3 = 1130 ± 80 a for H4 and 1340 ± 80 a for H5.

In all scenarios, our data suggest an IRD delivery shorter than the corresponding Greenland stadial duration, but longer than the 250 ± 150 a fresh water flux duration proposed in the model study on H4 from Roche et al. (2004). However, these authors did not rule out the possibility of two iceberg deliveries of ∼ 250 a separated by an AMOC resurgence lasting 400 a. In this case, the full event duration of 900 a appears close to our estimates.

3.6 Implication for HE triggering mechanisms

Mechanisms leading to HEs have been explored using conceptual to coupled climate models. Proposed triggers involve fresh-water fluxes (as reviewed by Kageyama et al., 2013), iceberg delivery in the North Atlantic Ocean (Jongma et al., 2013; Roberts et al.,

2014) and ice shelf collapse at the Laurentide margin (e.g., Alvarez-Solas et al., 2010; Marcott et al., 2011).

Our study clearly suggests that H4 and H5 happen after the beginning of GS-9 and GS-13 respectively, with a time lag of $140 \pm 40\,\mathrm{a}$ (H5) to $550 \pm 60\,\mathrm{a}$ (H4), i.e. when the North Atlantic region has already entered a cooling trend. This timing is in agreement with the hypothesis that progressive AMOC slow down and shoaling accompanied by sea ice extend isolate the sub-surface ocean from the cold atmosphere and produces a sub-surface warming (Rasmussen and Thomsen, 2004; Jonkers et al., 2010). In addition, this sub-surface warming could lead to a sea-level rise of ~ 0.5 to $1\,\mathrm{m}$ by reorganisation of the North Atlantic dynamic topography and by oceanic thermal expansion (as modelled in Shaffer et al., 2004; Flückiger et al., 2006). Both sub-surface warming and sea-level rise then contribute to destabilising ice shelves from the massive Laurentide ice sheet, causing the massive iceberg delivery of Heinrich events (Alvarez-Solas et al., 2010; Alvarez-Solas and Ramstein, 2011; Marcott et al., 2011).

Our results can contribute to create realistic scenarios to simulate Heinrich events. First, HEs do not start during full interstadial conditions but after the cooling trend of a Dansgaard–Oeschger cycle, when Greenland climate enters stadial conditions. Second, the end of the iceberg/fresh water perturbation likely occurs several centuries before Greenland abrupt warming.

3.7 Why does Greenland climate stay uniformly cold during the entire GS-9 and GS-13?

Atmospheric simulations (Li et al., 2010) suggest that Greenland temperature is sensitive to changes in sea ice cover anomalies in the Nordic Seas because of "a strengthening of the easterly flow over the Nordic Seas" impacting Central Greenland. On the contrary, in these simulations, NW Atlantic sea ice cover anomalies only affect the western flank of the Icelandic low and the associated atmospheric circulation anomaly does not noticeably impact Central Greenland. Supporting these results, the modelled regional pattern of Greenland warming in response to Nordic Seas sea-ice retreat is

in agreement with regional quantitative reconstruction of Greenland temperature and accumulation rate during MIS3 (Guillevic et al., 2013).

While we suggest large changes in the North Atlantic sea ice extent during H4, no specific sea ice change is depicted during this period as inferred from deep sea core records obtained from the Irminger Sea and south of the Faeroe Islands (Cortijo et al., 2005; Zumaque et al., 2012). However, bio-indicators in marine cores from the Norwegian Sea robustly record warmer temperature (e.g. based on foraminifers, Rasmussen and Thomsen, 2004; Dokken et al., 2013) and reduced sea ice cover (based on dinocysts, Eynaud et al., 2002) during stadials than during interstadials. To reconcile these conflicting model-data results, Rasmussen and Thomsen (2004) and Dokken et al. (2013) proposed a perennial sea-ice cover in the Norwegian Sea during all stadials of MIS3, separated by a halocline from warm waters of the North Atlantic Drift in subsurface, to where foraminifers might have moved their depth habitat. Dinocysts on the contrary may have stayed at the surface, and their observed assemblages could be due to productivity anomalies in zones of polynya. According to this scenario, the lack of specific sea ice anomaly in the Nordic Seas during GS-9 and GS-13 may explain why no cold anomaly is recorded in Greenland during H4 and H5.

Moreover, Rasmussen and Thomsen (2004), Dokken et al. (2013) and Petersen et al. (2013) proposed mechanisms that could explain why the Nordic Seas (and Greenland) remain in a stable stadial state while low to mid latitudes are gradually shifting towards interstadial conditions: during stadials, the heat advected along the North Atlantic Drift accumulates in sub-surface, below the sea ice in the Nordic Seas or below the ice shelf east of Greenland, until the low-density warm sub-surface water abruptly reaches the surface, thereby melting the sea-ice and/or ice shelf, which results in a rapid warming of the Nordic Seas (and Greenland).

Heinrich event 4 in Greenland ice core records

M. Guillevic et al.

4 Conclusions and perspectives

In summary, our new multi-proxy record from Greenland ice cores has revealed a 3 phase sequence of GS-9. While Greenland temperature remains uniformly cold along GS-9, synchronous changes in ^{17}O excess, MSA, δ^{18}O$_{atm}$, δD$-$CH$_4$, methane and CO$_2$ are interpreted as a polar ice core fingerprint of the low to mid latitude climatic impacts that we associate with H4. Following this interpretation, the beginning of the H4 impact on mid to low latitudes is dated at $39\,350 \pm 1\,520$ a b2k, 550 ± 60 a after the end of GI-9. It ends 740 ± 60 a later, when ^{17}O excess, MSA, δ^{18}O$_{atm}$ and δD$-$CH$_4$ have shifted back to interstadial climate values, 390 ± 50 a before the onset of GI-8. Preliminary investigations on GS-13 encompassing H5, based on the ice core proxies δ^{18}O, MSA, δ^{18}O$_{atm}$, CH$_4$ and CO$_2$ also reveal a 3 phase structure, as well as the same sequence of events (Fig. 7).

Our findings obviously call for systematic investigations of the ice core multi-proxy fingerprints of other Heinrich events, to assess the robustness of our results for H4 and H5, of mainly LIS origin, with respect to H3 and H6, mostly originating from European ice sheets (Hemming, 2004). The decoupling between the flat Greenland temperature during GS-9 and the climate variability associated with H4 at lower latitudes challenges the use of Greenland ice core temperatures as a single target for benchmarking climate simulations focused on HEs. Our multi-proxy study opens new paths for parallel investigations of different marine, terrestrial and ice core climate archives.

Appendix A: Synchronisation of the used ice cores to the GICC05 chronology

A1 Ice age scales

The GICC05 (Greenland Ice Core Chronology 2005) has been constructed for the NGRIP ice core from present back to 60 ka b2k based on annual layer counting in ice cores of parameters featuring seasonal scale variations (Vinther et al., 2006;

Full Screen / Esc

Printer-friendly Version

Interactive Discussion

Andersen et al., 2006; Rasmussen et al., 2006; Svensson et al., 2008). The GRIP, GISP2 (Seierstad et al., 2014) and NEEM ice cores (Rasmussen et al., 2013) have been synchronised to the NGRIP ice core using match points based on peaks of electrical conductivity and dielectrical properties of the ice. The synchronisation uncertainty between NGRIP, NEEM, GRIP and GISP2 is estimated to be $\sim 10\,\text{cm}$ (1 sigma, Rasmussen et al., 2013), resulting in $\sim 10\,\text{a}$ synchronisation uncertainty for GS-9. The GICC05 uncertainty is estimated by the maximum counting error in years (Rasmussen et al., 2006), with each uncertain year counted as $0.5 \pm 0.5\,\text{a}$. This can be considered as a $2\,\sigma$ uncertainty. We give the duration uncertainty of each of the phases of GS-9 and GS-13 as the sum of the uncertain years counted within each phase.

A2 Gas age scales

For the NGRIP gas records ($\delta\text{D}-\text{CH}_4$, $\delta^{18}\text{O}_{\text{atm}}$), we use the gas age scale from Kindler et al. (2014), initially constructed on the NGRIP ss09sea06bm timescale (NGRIP members, 2004; Wolff et al., 2010), and we transfer it to the GICC05 chronology. We use the NEEM gas age scale from Guillevic et al. (2013) for GS-8 to GS-12, compatible with the later release from Rasmussen et al. (2013), and the one from Rasmussen et al. (2013) for GI-12 to GI-14. The NGRIP and NEEM gas age scale covering GS-9 are well constrained (ice-gas synchronisation uncertainty less than 100 years for NEEM, less than 160 years for NGRIP) thanks to numerous measured $\delta^{15}\text{N}$ data (Kindler et al., 2014; Guillevic et al., 2013; Rasmussen et al., 2013).

To synchronise the Byrd gas records to the NEEM ice core, we use a traditional approach consisting in matching methane records from both ice cores (Blunier et al., 1998). We first use the high resolution NEEM methane record on its GICC05 gas age scale (Guillevic et al., 2013). We then match the Byrd methane record (Ahn et al., 2012) to the NEEM methane record, using as match points the mid-slope of each GI onset (Fig. 8 and Table 2). We perform a linear interpolation in between the match points. We then apply the obtain depth-gas age scale for Byrd to the Byrd CO_2 record.

The same method is applied to the Siple Dome methane record in order to place the Siple Dome $\delta^{18}O_{atm}$ record (Severinghaus et al., 2009) on the GICC05 timescale, to compare with our NEEM $\delta^{18}O_{atm}$ record (Fig. 9 and Table 2).

References

Abram, N. J., Wolff, E. W., and Curran, M. A.: A review of sea ice proxy information from polar ice cores, Quaternary Sci. Rev., 79, 168–183, doi:10.1016/j.quascirev.2013.01.011, 2013. 1189

Ahn, J. and Brook, E. J.: Atmospheric CO_2 and climate on millennial time scales during the last glacial period, Science, 322, 83–85, doi:10.1126/science.1160832, 2008. 1213

Ahn, J., Brook, E., Schmittner, A., and Kreutz, K.: Abrupt change in atmospheric CO_2 during the last ice age, Geophys. Res. Lett., 39, L18771, doi:10.1029/2012GL053018, 2012. 1190, 1193, 1198, 1213, 1217, 1220, 1221, 1222

Alvarez-Solas, J. and Ramstein, G.: On the triggering mechanism of Heinrich events, P. Natl. Acad. Sci. USA, 108, E1359–E1360, doi:10.1073/pnas.1116575108, 2011. 1195

Alvarez-Solas, J., Charbit, S., Ritz, C., Paillard, D., Ramstein, G., and Dumas, C.: Links between ocean temperature and iceberg discharge during Heinrich events, Nat. Geosci., 3, 122–126, doi:10.1038/NGEO752, 2010. 1195

Andersen, K. K., Svensson, A., Johnsen, S. J., Rasmussen, S. O., Bigler, M., Röthlisberger, R., Ruth, U., Siggaard-Andersen, M.-L., Steffensen, J. P., Dahl-Jensen, D., Vinther, B. M., and Clausen, H. B.: The Greenland Ice Core Chronology 2005, 15–42 ka. Part 1: constructing the time scale, Quaternary Sci. Rev., 25, 3246–3257, doi:10.1016/j.quascirev.2006.08.002, 2006. 1198

Anderson, R. F., Ali, S., Bradtmiller, L. I., Nielsen, S. H. H., Fleisher, M. Q., Anderson, B. E., and Burckle, L. H.: Wind-driven upwelling in the Southern Ocean and the deglacial rise in atmospheric CO_2, Science, 323, 1443–1448, doi:10.1126/science.1167441, 2009. 1190

Auffret, G., Zaragosi, S., Dennielou, B., Cortijo, E., Rooij, D. V., Grousset, F., Pujol, C., Eynaud, F., and Siegert, M.: Terrigenous fluxes at the Celtic margin during the last glacial cycle, Mar. Geol., 188, 79–108, doi:10.1016/S0025-3227(02)00276-1, 2002. 1219

Austin, W. E. and Hibbert, F. D.: Tracing time in the ocean: a brief review of chronological constraints (60–8 kyr) on North Atlantic marine event–based stratigraphies, Quaternary Sci. Rev., 36, 28–37, doi:10.1016/j.quascirev.2012.01.015, 2012. 1182

Baumgartner, M., Schilt, A., Eicher, O., Schmitt, J., Schwander, J., Spahni, R., Fischer, H., and Stocker, T. F.: High-resolution interpolar difference of atmospheric methane around the Last Glacial Maximum, Biogeosciences, 9, 3961–3977, doi:10.5194/bg-9-3961-2012, 2012. 1181

Bazin, L., Landais, A., Lemieux-Dudon, B., Toyé Mahamadou Kele, H., Veres, D., Parrenin, F., Martinerie, P., Ritz, C., Capron, E., Lipenkov, V., Loutre, M.-F., Raynaud, D., Vinther, B., Svensson, A., Rasmussen, S. O., Severi, M., Blunier, T., Leuenberger, M., Fischer, H., Masson-Delmotte, V., Chappellaz, J., and Wolff, E.: An optimized multi-proxy, multi-site Antarctic ice and gas orbital chronology (AICC2012): 120–800 ka, Clim. Past, 9, 1715–1731, doi:10.5194/cp-9-1715-2013, 2013. 1214, 1220

Bender, M., Sowers, T., Dickinson, M., Orchado, J., Grootes, P., Mayewski, P., and Meese, D.: Climate correlations between Greenland and Antarctica during the past 100 000 years, Nature, 372, 663–666, doi:10.1038/372663a0, 1994a. 1189

Bender, M., Sowers, T., and Labeyrie, L.: The Dole effect and its variations during the last 130,000 years as measured in the Vostok ice core, Global Biogeochem. Cy., 8, 363–376, doi:10.1029/94GB00724, 1994b. 1181

Bereiter, B., Lüthi, D., Siegrist, M., Schüpbach, S., Stocker, T. F., and Fischer, H.: Mode change of millennial CO_2 variability during the last glacial cycle associated with a bipolar marine carbon seesaw, P. Natl. Acad. Sci. USA, 109, 9755–9760, doi:10.1073/pnas.1204069109, 2012. 1193, 1220

Heinrich event 4 in Greenland ice core records

M. Guillevic et al.

Title Page

Abstract · Introduction

Conclusions · References

Tables · Figures

◄ · ►

◄ · ►

Back · Close

Full Screen / Esc

Printer-friendly Version

Interactive Discussion

Blunier, T., Chappellaz, J., Schwander, J., Dällenbach, A., Stauffer, B., Stocker, T., Raynaud, D., Jouzel, J., Clausen, H., Hammer, C., and Johnsen, S.: Asynchrony of Antarctic and Greenland climate change during the last glacial period, Nature, 394, 739–743, doi:10.1038/29447, 1998. 1198

5 Boch, R., Cheng, H., Spötl, C., Edwards, R. L., Wang, X., and Häuselmann, P.: NALPS: a precisely dated European climate record 120–60 ka, Clim. Past, 7, 1247–1259, doi:10.5194/cp-7-1247-2011, 2011. 1181

Bock, M., Schmitt, J., Möller, L., Spahni, R., Blunier, T., and Fischer, H.: Hydrogen isotopes preclude marine hydrate CH_4 emissions at the onset of Dansgaard-Oeschger events, Science, 328, 1686–1689, doi:10.1126/science.1187651, 2010. 1189, 1190, 1217

10 Bond, G., Heinrich, H., Broecker, W., Labeyrie, L., McManus, J., Andrews, J., Huon, S., Jantschik, R., Clasen, S., Simet, C., Tedesco, K., Klas, M., Bonani, G., and Ivy, S.: Evidence for massive discharges of icebergs into the North Atlantic ocean during the last glacial period, Nature, 360, 245–249, 1992. 1182

15 Bond, G., Broecher, W., Johnsen, S. J., MacManus, J., Laberie, L., Jouzel, J., and Bonani, G.: Correlations between climate records from North Atlantic sediments and Greenland ice, Nature, 365, 143–147, doi:10.1038/365143a0, 1993. 1182

Bondevik, S., Mangerud, J., Birks, H. H., Gulliksen, S., and Reimer, P.: Changes in north Atlantic radiocarbon reservoir ages during the Allerød and Younger Dryas, Science, 312, 1514–1517, doi:10.1126/science.1123300, 2006. 1183

20 Brook, E. J., White, J. W., Schilla, A. S., Bender, M. L., Barnett, B., Severinghaus, J. P., Taylor, K. C., Alley, R. B., and Steig, E. J.: Timing of millennial-scale climate change at Siple Dome, West Antarctica, during the last glacial period, Quaternary Sci. Rev., 24, 1333–1343, doi:10.1016/j.quascirev.2005.02.002, 2005. 1213, 1222

25 Buiron, D., Chappellaz, J., Stenni, B., Frezzotti, M., Baumgartner, M., Capron, E., Landais, A., Lemieux-Dudon, B., Masson-Delmotte, V., Montagnat, M., Parrenin, F., and Schilt, A.: TALDICE-1 age scale of the Talos Dome deep ice core, East Antarctica, Clim. Past, 7, 1–16, doi:10.5194/cp-7-1-2011, 2011. 1220

Capron, E., Landais, A., Chappellaz, J., Schilt, A., Buiron, D., Dahl-Jensen, D., Johnsen, S. J., 30 Jouzel, J., Lemieux-Dudon, B., Loulergue, L., Leuenberger, M., Masson-Delmotte, V., Meyer, H., Oerter, H., and Stenni, B.: Millennial and sub-millennial scale climatic variations recorded in polar ice cores over the last glacial period, Clim. Past, 6, 345–365, doi:10.5194/cp-6-345-2010, 2010. 1181

Title Page

Abstract | Introduction

Conclusions | References

Tables | Figures

|◀ | ▶|

◀ | ▶

Back | Close

Full Screen / Esc

Printer-friendly Version

Interactive Discussion

Chappellaz, J., Blunier, T., Raynaud, D., Barnola, J., Schwander, J., and Stauffer, B.: Synchronous changes in atmospheric CH_4 and Greenland climate between 40 and 8 kyr BP, Nature, 366, 443–445, doi:10.1038/366443a0, 1993. 1181

Chappellaz, J., Stowasser, C., Blunier, T., Baslev-Clausen, D., Brook, E. J., Dallmayr, R., Faïn, X., Lee, J. E., Mitchell, L. E., Pascual, O., Romanini, D., Rosen, J., and Schüpbach, S.: High-resolution glacial and deglacial record of atmospheric methane by continuous-flow and laser spectrometer analysis along the NEEM ice core, Clim. Past, 9, 2579–2593, doi:10.5194/cp-9-2579-2013, 2013. 1181, 1189, 1193, 1213, 1217, 1220, 1221, 1222

Chiang, J. C. H., Cheng, W., and Bitz, C. M.: Fast teleconnections to the tropical Atlantic sector from Atlantic thermohaline adjustment, Geophys. Res. Lett., 35, L07704, doi:10.1029/2008GL033292, 2008. 1183, 1189, 1192

Clement, A. C. and Peterson, L. C.: Mechanisms of abrupt climate change of the last glacial period, Rev. Geophys., 46, RG4002, doi:10.1029/2006RG000204, 2008. 1181, 1182

Cortijo, E., Duplessy, J.-C., Labeyrie, L., Duprat, J., and Paillard, D.: Heinrich events: hydrological impact, CR Geosci., 337, 897–907, doi:10.1016/j.crte.2005.04.011, 2005. 1196

Cvijanovic, I. and Chiang, J.: Global energy budget changes to high latitude North Atlantic cooling and the tropical ITCZ response, Clim. Dynam., 40, 1435–1452, doi:10.1007/s00382-012-1482-1, 2013. 1183

Dahl-Jensen, D. and NEEM community members: Eemian interglacial reconstructed from a Greenland folded ice core, Nature, 493, 489–494, doi:10.1038/nature11789, 2013. 1185

Dansgaard, W.: Stable isotopes in precipitation, Tellus, 16, 436–468, doi:10.1111/j.2153-3490.1964.tb00181.x, 1964. 1184

de Abreu, L., Shackleton, N. J., Schönfeld, J., Hall, M., and Chapman, M.: Millennial-scale oceanic climate variability off the Western Iberian margin during the last two glacial periods, Mar. Geol., 196, 1–20, doi:10.1016/S0025-3227(03)00046-X, 2003. 1191, 1219

Dickson, A. J., Austin, W. E. N., Hall, I. R., Maslin, M. A., and Kucera, M.: Centennial-scale evolution of Dansgaard-Oeschger events in the northeast Atlantic Ocean between 39.5 and 56.5 ka BP, Paleoceanography, 23, PA3206, doi:10.1029/2008PA001595, 2008. 1191, 1219

Dokken, T. M., Nisancioglu, K. H., Li, C., Battisti, D. S., and Kissel, C.: Dansgaard-Oeschger cycles: Interactions between ocean and sea ice intrinsic to the Nordic seas, Paleoceanography, 28, 1–12, doi:10.1002/palo.20042, 2013. 1196

EPICA community members: One-to-one coupling of glacial climate variability in Greenland and Antarctica, Nature, 444, 195–198, doi:10.1038/nature05301, 2006. 1181

Heinrich event 4 in Greenland ice core records

M. Guillevic et al.

Title Page

Abstract | Introduction

Conclusions | References

Tables | Figures

|◀ | ▶|

◀ | ▶

Back | Close

Full Screen / Esc

Printer-friendly Version

Interactive Discussion

Eynaud, F., Turon, J., Matthiessen, J., Kissel, C., Peypouquet, J., de Vernal, A., and Henry, M.: Norwegian sea-surface palaeoenvironments of marine oxygen-isotope stage 3: the paradoxical response of dinoflagellate cysts, J. Quaternary Sci., 17, 349–359, doi:10.1002/jqs.676, 2002. 1196

Eynaud, F., de Abreu, L., Voelker, A., Schönfeld, J., Salgueiro, E., Turon, J.-L., Penaud, A., Toucanne, S., Naughton, F., ni, M. F. S.-G., Malaizé, B., and Cacho, I.: Position of the Polar Front along the western Iberian margin during key cold episodes of the last 45 ka, Geochem. Geophy. Geosy., 10, Q07U05, doi:10.1029/2009GC002398, 2009. 1219

Eynaud, F., Malaizé, B., Zaragosi, S., de Vernal, A., Scourse, J., Pujol, C., Cortijo, E., Grousset, F. E., Penaud, A., Toucanne, S., Turon, J.-L., and Auffret, G.: New constraints on European glacial freshwater releases to the North Atlantic Ocean, Geophys. Res. Lett., 39, L15601, doi:10.1029/2012GL052100, 2012. 1182, 1214

Fleitmann, D., Treble Jr., P., F. C., Cole, J., and Cobb, K.: White Paper: Speleothem-based climate proxy records, in: PAGES/CLIVAR Proxy Uncertainty Workshop in Trieste, available at: http://pages-igbp.org/products/meeting-products/2032-white-paper-speleothem-based-climate-proxy-records (last access: 29 January 2014), 2008. 1183

Flückiger, J., Knutti, R., and White, J. W. C.: Oceanic processes as potential trigger and amplifying mechanisms for Heinrich events, Paleoceanography, 21, PA2014, doi:10.1029/2005PA001204, 2006. 1182, 1195

Genty, D., Combourieu-Nebout, N., Peyron, O., Blamart, D., Wainer, K., Mansuri, F., Ghaleb, B., Isabello, L., Dormoy, I., von Grafenstein, U., Bonelli, S., Landais, A., and Brauer, A.: Isotopic characterization of rapid climatic events during OIS3 and OIS4 in Villars Cave stalagmites (SW-France) and correlation with Atlantic and Mediterranean pollen records, Quaternary Sci. Rev., 29, 2799–2820, doi:10.1016/j.quascirev.2010.06.035, 2010. 1181

Grousset, F., Labeyrie, L., Sinko, J., Cremer, M., Bond, G., Duprat, J., Cortijo, E., and Huon, S.: Patterns of ice-rafted detritus in the glacial North Atlantic (40–55° N), Paleoceanography, 8, 175–192, doi:10.1029/92PA02923, 1993. 1182

Grousset, F., Pujol, C., Labeyrie, L., Auffret, G., and Boelaert, A.: Were the North Atlantic Heinrich events triggered by the behavior of the European ice sheets?, Geology, 28, 123–126, doi:10.1130/0091-7613(2000)28<123:WTNAHE>2.0.CO;2, 2000. 1182

Guillevic, M., Bazin, L., Landais, A., Kindler, P., Orsi, A., Masson-Delmotte, V., Blunier, T., Buchardt, S. L., Capron, E., Leuenberger, M., Martinerie, P., Prié, F., and Vinther, B. M.:

Heinrich event 4 in Greenland ice core records

M. Guillevic et al.

Spatial gradients of temperature, accumulation and δ^{18}O-ice in Greenland over a series of Dansgaard–Oeschger events, Clim. Past, 9, 1029–1051, doi:10.5194/cp-9-1029-2013, 2013. 1187, 1188, 1196, 1198, 1213, 1217, 1221, 1222

Gwiazda, R., Hemming, S., and Broecker, W.: Provenance of icebergs during Heinrich Event 3 and the contrast to their sources during other Heinrich episodes, Paleoceanography, 11, 371–378, doi:10.1029/96PA01022, 1996. 1182

Heinrich, H.: Origin and consequences of cyclic ice rafting in the Northeast Atlantic Ocean during the past 130,000 years, Quaternary Res., 29, 142–152, doi:10.1016/0033-5894(88)90057-9, 1988. 1182

Hemming, S., Broecker, W., Sharp, W., Bond, G., Gwiazda, R., McManus, J., Klas, M., and Hajdas, I.: Provenance of the Heinrich layers in core V28-82, northeastern Atlantic, ^{40}Ar-^{39}Ar ages of ice-rafted hornblende, Pb isotopes in feldspar grains, and Nd-Sr-Pb isotopes in the fine sediment fraction, Earth Planet. Sc. Lett., 164, 317–333, doi:10.1016/S0012-821X(98)00224-6, 1998. 1182

Hemming, S. R.: Heinrich events: massive Late Pleistocene detritus layers of the North Atlantic and their global climate imprint, Rev. Geophys., 42, RG1005, doi:10.1029/2003RG000128, 2004. 1182, 1183, 1185, 1193, 1194, 1197, 1215

Hoffmann, G., Cuntz, M., Weber, C., Ciais, P., Friedlingstein, P., Heimann, M., Jouzel, J., Kaduk, J., Maier-Reimer, E., Seibt, U., and Six, K.: A model of the Earth's Dole effect, Global Biogeochem. Cy., 18, GB1008, doi:10.1029/2003GB002059, 2004. 1189

Hopcroft, P. O., Valdes, P. J., and Beerling, D. J.: Simulating idealized Dansgaard-Oeschger events and their potential impacts on the global methane cycle, Quaternary Sci. Rev., 30, 3258–3268, doi:10.1016/j.quascirev.2011.08.012, 2011. 1190

Huber, C., Leuenberger, M., Spahni, R., Flückiger, J., Schwander, J., Stocker, T. F., Johnsen, S. J., Landais, A., and Jouzel, J.: Isotope calibrated Greenland temperature record over Marine Isotope Stage 3 and its relation to CH$_4$, Earth Planet. Sc. Lett., 243, 504–519, doi:10.1016/j.epsl.2006.01.002, 2006. 1193, 1220

Itambi, A., von Dobeneck, T., Mulitza, S., Bickert, T., and Heslop, D.: Millennial-scale northwest African droughts related to Heinrich events and Dansgaard-Oeschger cycles: Evidence in marine sediments from offshore Senegal, Paleoceanography, 24, PA1205, doi:10.1029/2007PA001570, 2009. 1190

Johnsen, S. J., Dansgaard, W., and White, J. W. C.: The origin of Arctic precipitation under present and glacial climate, Tellus B, 41, 452–468, doi:10.1111/j.1600-0889.1989.tb00321.x, 1989. 1188

Jongma, J. I., Renssen, H., and Roche, D. M.: Simulating Heinrich event 1 with interactive icebergs, Clim. Dynam., 40, 1373–1385, doi:10.1007/s00382-012-1421-1, 2013. 1194

Jonkers, L., Moros, M., Prins, M. A., Dokken, T., Dahl, C. A., Dijkstra, N., Perner, K., and Brummer, G.-J. A.: A reconstruction of sea surface warming in the northern North Atlantic during MIS 3 ice-rafting events, Quaternary Sci. Rev., 29, 1791–1800, doi:10.1016/j.quascirev.2010.03.014, 2010. 1195

Jouzel, J., Stiévenard, N., Johnsen, S., Landais, A., Masson-Delmotte, V., Sveinbjörnsdóttir, A., Vimeux, F., von Grafenstein, U., and White, J.: The GRIP deuterium-excess record, Quaternary Sci. Rev., 26, 1–17, doi:10.1016/j.quascirev.2006.07.015, 2007. 1188, 1193

Jullien, E., Grousset, F. E., Hemming, S. R., Peck, V. L., Hall, I. R., Jeantet, C., and Billy, I.: Contrasting conditions preceding MIS3 and MIS2 Heinrich events, Global Planet. Change, 54, 225–238, doi:10.1016/j.gloplacha.2006.06.021, 2006. 1182, 1185

Jullien, E., Grousset, F., Malaizé, B., Duprat, J., Sanchez-Goni, M. F., Eynaud, F., Charlier, K., Schneider, R., Bory, A., Bout, V., and Flores, J. A.: Low-latitude dusty events vs. high-latitude icy Heinrich events, Quaternary Res., 68, 279–386, doi:10.1016/j.yqres.2007.07.007, 2007. 1190

Kageyama, M., Merkel, U., Otto-Bliesner, B., Prange, M., Abe-Ouchi, A., Lohmann, G., Ohgaito, R., Roche, D. M., Singarayer, J., Swingedouw, D., and Zhang, X.: Climatic impacts of fresh water hosing under Last Glacial Maximum conditions: a multi-model study, Clim. Past, 9, 935–953, doi:10.5194/cp-9-935-2013, 2013. 1182, 1194

Kanner, L. C., Burns, S. J., Cheng, H., and Edwards, R. L.: High-latitude forcing of the South American summer monsoon during the Last Glacial, Science, 335, 570–573, doi:10.1126/science.1213397, 2012. 1183

Kindler, P., Guillevic, M., Baumgartner, M., Schwander, J., Landais, A., and Leuenberger, M.: NGRIP temperature reconstruction from 10 to 120 kyr b2k, Clim. Past Discuss., 9, 4099–4143, doi:10.5194/cpd-9-4099-2013, 2013. 1184, 1198

Landais, A., Masson-Delmotte, V., Nebout, N. C., Jouzel, J., Blunier, T., Leuenberger, M., Dahl-Jensen, D., and Johnsen, S.: Millenial scale variations of the isotopic composition of atmospheric oxygen over Marine Isotopic Stage 4, Earth Planet. Sc. Lett., 258, 101–113, doi:10.1016/j.epsl.2007.03.027, 2007. 1181

Heinrich event 4 in Greenland ice core records

M. Guillevic et al.

⏮ | ⏭

◀ | ▶

Back | Close

Full Screen / Esc

Printer-friendly Version

Interactive Discussion

Landais, A., Dreyfus, G., Capron, E., Masson-Delmotte, V., Sanchez-Goni, M., Desprat, S., Hoffmann, G., Jouzel, J., Leuenberger, M., and Johnsen, S.: What drives the millennial and orbital variations of $\delta^{18}O_{atm}$?, Quaternary Sci. Rev., 29, 235–246, doi:10.1016/j.quascirev.2009.07.005, 2010. 1187, 1189

Landais, A., Steen-Larsen, H., Guillevic, M., Masson-Delmotte, V., Vinther, B., and Winkler, R.: Triple isotopic composition of oxygen in surface snow and water vapor at NEEM (Greenland), Geochim. Cosmochim. Ac., 77, 304–316, doi:10.1016/j.gca.2011.11.022, 2012. 1184

Lewis, S. C., LeGrande, A. N., Kelley, M., and Schmidt, G. A.: Water vapour source impacts on oxygen isotope variability in tropical precipitation during Heinrich events, Clim. Past, 6, 325–343, doi:10.5194/cp-6-325-2010, 2010. 1189, 1190

Li, C., Battisti, D., and Bitz, C.: Can North Atlantic sea ice anomalies account for Dansgaard-Oeschger climate signals?, J. Climate, 23, 5457–5475, doi:10.1175/2010JCLI3409.1, 2010. 1195

Luz, B. and Barkan, E.: The isotopic ratios $^{17}O/^{16}O$ and $^{18}O/^{16}O$ in molecular oxygen and their significance in biogeochemistry, Geochim. Cosmochim. Ac., 69, 1099–1110, doi:10.1016/j.gca.2004.09.001, 2005. 1185

Luz, B., Barkan, E., Yam, R., and Shemesh, A.: Fractionation of oxygen and hydrogen isotopes in evaporating water, Geochim. Cosmochim. Ac., 73, 6697–6703, doi:10.1016/j.gca.2009.08.008, 2009. 1186

Marcott, S. A., Clark, P. U., Padman, L., Klinkhammer, G. P., Springer, S. R., Liu, Z., Otto-Bliesner, B. L., Carlson, A. E., Ungerer, A., Padman, J., He, F., Cheng, J., and Schmittner, A.: Ice-shelf collapse from subsurface warming as a trigger for Heinrich events, P. Natl. Acad. Sci. USA, 108, 13415–13419, doi:10.1073/pnas.1104772108, 2011. 1182, 1195

Masson-Delmotte, V., Jouzel, J., Landais, A., Stiévenard, M., Johnsen, S. J., White, J. W. C., Werner, M., Sveinbjörnsdóttir, A., and Fuhrer, K.: GRIP deuterium excess reveals rapid and orbital-scale changes in Greenland moisture origin, Science, 309, 118–121, doi:10.1126/science.1108575, 2005. 1184, 1188, 1193

Menviel, L., England, M., Meissner, K., Mouchet, A., and Yu, J.: Atlantic-Pacific seesaw and its role in outgassing CO_2 during Heinrich events, Paleoceanography, 29, 1–13, doi:10.1002/2013PA002542, 2014. 1190

Möller, L., Sowers, T., Bock, M., Spahni, R., Behrens, M., Schmitt, J., Miller, H., and Fischer, H.: Independent variations of CH_4 emissions and isotopic composition over the past 160,000 years, Nat. Geosci., 6, 885–890, doi:10.1038/ngeo1922, 2013. 1190

Heinrich event 4 in Greenland ice core records

M. Guillevic et al.

Title Page

Abstract | Introduction

Conclusions | References

Tables | Figures

|◄ | ►|

◄ | ►

Back | Close

Full Screen / Esc

Printer-friendly Version

Interactive Discussion

Mosblech, N. A., Bush, M. B., Gosling, W. D., Hodell, D., Thomas, L., van Calsteren, P., Correa-Metrio, A., Valencia, B. G., Curtis, J., and van Woesik, R.: North Atlantic forcing of Amazonian precipitation during the last ice age, Nat. Geosci., 5, 817–820, doi:10.1038/ngeo1588, 2012. 1183

5 Mulitza, S., Prange, M., Stuut, J.-B., Zabel, M., von Dobeneck, T., Itambi, A. C., Nizou, J., Schulz, M., and Wefer, G.: Sahel megadroughts triggered by glacial slowdowns of Atlantic meridional overturning, Paleoceanography, 23, PA4206, doi:10.1029/2008PA001637, 2008. 1182, 1190

Naughton, F., Sánchez Goñi, M.F., Kageyama, M., Bard, E., Duprat, J., Cortijo, E., De-
10 sprat, S., Malaizé, B., Joly, C., Rostek, F., and Turon, J.-L.: Wet to dry climatic trend in north-western Iberia within Heinrich events, Earth Planet. Sc. Lett., 284, 329–342, doi:10.1016/j.epsl.2009.05.001, 2009. 1191

NGRIP members: High-resolution record of Northern Hemisphere climate extending into the last interglacial period, Nature, 431, 147–151, doi:10.1038/nature02805, 2004. 1181, 1185,
15 1198, 1214

O'Dwyer, J., Isaksson, E., Vinje, T., Jauhiainen, T., Moore, J., Pohjola, V., Vaikmae, R., and van de Wal, R.: Methanesulfonic acid in a Svalbard ice core as an indicator of ocean climate, Geophys. Res. Lett., 27, 1159–1162, doi:10.1029/1999gl011106, 2000. 1189

Otto-Bliesner, B. L. and Brady, E. C.: The sensitivity of the climate response to the magnitude
20 and location of freshwater forcing: last glacial maximum experiments, Quaternary Sci. Rev., 29, 56–73, doi:10.1016/j.quascirev.2009.07.004, 2010. 1194

Pausata, F. S. R., Battisti, D. S., Nisancioglu, K. H., and Bitz, C. M.: Chinese stalagmite δ^{18}O controlled by changes in the Indian monsoon during a simulated Heinrich event, Nat. Geosci., 4, 474–480, doi:10.1038/NGEO1169, 2011. 1189, 1190

25 Peters, C., Walden, J., and Austin, W. E. N.: Magnetic signature of European margin sed-iments: Provenance of ice-rafted debris and the climatic response of the British ice sheet during Marine Isotope Stages 2 and 3, J. Geophys. Res.-Earth, 113, F03007, doi:10.1029/2007JF000836, 2008. 1182, 1191, 1219

Petersen, S. V., Schrag, D. P., and Clark, P. U.: A new mechanism for Dansgaard-Oeschger
30 cycles, Paleoceanography, 28, 24–30, doi:10.1029/2012PA002364, 2013. 1196

Peterson, L. C., Haug, G. H., Hughen, K. A., and Röhl, U.: Rapid changes in the hy-drologic cycle of the tropical Atlantic during the Last Glacial, Science, 290, 1947–1951, doi:10.1126/science.290.5498.1947, 2000. 1181

Heinrich event 4 in Greenland ice core records

M. Guillevic et al.

Title Page

Abstract | Introduction

Conclusions | References

Tables | Figures

◀◀ | ▶▶

◀ | ▶

Back | Close

Full Screen / Esc

Printer-friendly Version

Interactive Discussion

Rashid, H., Hesse, R., and Piper, D.: Evidence for an additional Heinrich event between H5 and H6 in the Labrador Sea, Paleoceanography, 18, 1077, doi:10.1029/2003PA000913, 2003. 1182, 1214

Rasmussen, S. O., Andersen, K. K., Svensson, A. M., Steffensen, J. P., Vinther, B. M., Clausen, H. B., Siggaard-Andersen, M.-L., Johnsen, S. J., Larsen, L. B., Dahl-Jensen, D., Bigler, M., Röthlisberger, R., Fischer, H., Goto-Azuma, K., Hansson, M. E., and Ruth, U.: A new Greenland ice core chronology for the last glacial termination, J. Geophys. Res., 111, D06102, doi:10.1029/2005JD006079, 2006. 1198, 1212

Rasmussen, S. O., Abbott, P. M., Blunier, T., Bourne, A. J., Brook, E., Buchardt, S. L., Buizert, C., Chappellaz, J., Clausen, H. B., Cook, E., Dahl-Jensen, D., Davies, S. M., Guillevic, M., Kipfstuhl, S., Laepple, T., Seierstad, I. K., Severinghaus, J. P., Steffensen, J. P., Stowasser, C., Svensson, A., Vallelonga, P., Vinther, B. M., Wilhelms, F., and Winstrup, M.: A first chronology for the North Greenland Eemian Ice Drilling (NEEM) ice core, Clim. Past, 9, 2713–2730, doi:10.5194/cp-9-2713-2013, 2013. 1198, 1212, 1213

Rasmussen, S., Bigler, M., Blockley, S., Blunier, T., Buchardt, S. L., Clausen, H. B., Cvijanovic, I., Dahl-Jensen, D., Johnsen, S. J., Fischer, H., Gkinis, V., Guillevic, M., Hoek, W., Lowe, J. J., Pedro, J., Popp, T., Seierstad, I. E., Steffensen, J., Svensson, A. M., Vallelonga, P., Vinther, B. M., Walker, M. J., Wheatley, J., and Winstrup, M.: A stratigraphic framework for robust naming and correlation of past abrupt climatic changes during the last glacial period based on three synchronized Greenland ice core records, Quaternary Sci. Rev., submitted, 2014. 1212

Rasmussen, T. L. and Thomsen, E.: The role of the North Atlantic Drift in the millennial timescale glacial climate fluctuations, Palaeogeogr. Palaeocl., 210, 101–116, doi:10.1016/j.palaeo.2004.04.005, 2004. 1195, 1196

Rasmussen, T., Oppo, D., Thomsen, E., and Lehman, S.: Deep sea records from the southeast Labrador Sea: Ocean circulation changes and ice-rafting events during the last 160,000 years, Paleoceanography, 18, 1018, doi:10.1029/2001PA000736, 2003. 1182, 1214

Risi, C., Landais, A., Bony, S., Jouzel, J., Masson-Delmotte, V., and Vimeux, F.: Understanding the ^{17}O excess glacial-interglacial variations in Vostok precipitation, J. Geophys. Res.-Atmos., 115, D10112, doi:10.1029/2008JD011535, 2010. 1188

Ritz, S. P., Stocker, T. F., and Müller, S. A.: Modeling the effect of abrupt ocean circulation change on marine reservoir age, Earth Planet. Sc. Lett., 268, 202–211, doi:10.1016/j.epsl.2008.01.024, 2008. 1183

Heinrich event 4 in Greenland ice core records

M. Guillevic et al.

Title Page

Abstract | Introduction

Conclusions | References

Tables | Figures

|◀ | ▶|

◀ | ▶

Back | Close

Full Screen / Esc

Printer-friendly Version

Interactive Discussion

Roberts, W., Valdes, P., and Payne, A.: A new constraint on the sixe of Heinrich Events from an iceberg/sediment model, Earth Planet. Sc. Lett., 386, 1–9, doi:10.1016/j.epsl.2013.10.020, 2014. 1194

Roche, D., Paillard, D., and Cortijo, E.: Constraints on the duration and freshwater release of Heinrich event 4 through isotope modelling, Nature, 432, 379–382, doi:10.1038/nature03059, 2004. 1182, 1194

Roche, D., Wiersma, A., and Renssen, H.: A systematic study of the impact of freshwater pulses with respect to different geographical locations, Climate Dyn., 34, 997–1013, doi:10.1007/s00382-009-0578-8, 2010. 1194

Ruddiman, W. F.: Late Quaternary deposition of ice-rafted sand in the subpolar North Atlantic (lat 40 to 65N), Geol. Soc. Am. Bull., 88, 1813–1827, doi:10.1130/0016-7606(1977)88<1813:LQDOIS>2.0.CO;2, 1977. 1182, 1191

Saltzman, E., Whung, P.-Y., and Mayewski, P.: Methanesulfonate in the Greenland Ice Sheet Project 2 ice core, J. Geophys. Res., 102, 26649–26657, doi:10.1029/97JC01377, 1997. 1189, 1193, 1217, 1220

Sánchez Goñi, M. and Harrison, S.: Millennial-scale climate variability and vegetation changes during the Last Glacial: Concepts and terminology, Quaternary Sci. Rev., 29, 2823–2827, doi:10.1016/j.quascirev.2009.11.014, 2010. 1181, 1182, 1214

Sánchez-Goñi, M., Landais, A., Fletcher, W. J., Naughton, F., Desprat, S., and Duprat, J.: Contrasting impacts of Dansgaard–Oeschger events over a western European latitudinal transect modulated by orbital parameters, Quaternary Sci. Rev., 27, 1136–1151, doi:10.1016/j.quascirev.2008.03.003, 2008. 1219

Schoenemann, S. W., Schauer, A. J., and Steig, E. J.: Measurement of SLAP2 and GISP δ^{17}O and proposed VSMOW-SLAP normalization for δ^{17}O and $^{17}O_{excess}$, Rapid Commun. Mass Sp., 27, 582–590, doi:10.1002/rcm.6486, 2013. 1186

Seierstad, I. K., Abbott, P., Bigler, M., Blunier, T., Bourne, A., Brook, E., Buchardt, S. L., Buizert, C., Clausen, H. B., Cook, E., Dahl-Jensen, D., Davies, S., Guillevic, M., Johnsen, S. J., Pedersen, D. S., Popp, T. J., Rasmussen, S. O., Severinghaus, J., Svensson, A., and Vinther, B. M.: Consistently dated records from the Greenland GRIP, GISP2 and NGRIP ice cores for the past 104 ka reveal regional millennial-scale isotope gradients with possible Heinrich Event imprint, Quaternary Sci. Rev., submitted, 2014. 1198

Heinrich event 4 in Greenland ice core records

M. Guillevic et al.

Severinghaus, J., Beaudette, R., Headly, M. A., Taylor, K., and Brook, E. J.: Oxygen-18 of O_2 records the impact of abrupt climate change on the terrestrial biosphere, Science, 324, 1431–1434, doi:10.1126/science.1169473, 2009. 1181, 1183, 1187, 1189, 1199, 1222

Shaffer, G., Olsen, S. M., and Bjerrum, C. J.: Ocean subsurface warming as a mechanism for coupling Dansgaard-Oeschger climate cycles and ice-rafting events, Geophys. Res. Lett., 31, L24202, doi:10.1029/2004GL020968, 2004. 1195

Sharma, S., Chan, E., Ishizawa, M., Toom-Sauntry, D., Gong, S. L., Li, S. M., Tarasick, D. W., Leaitch, W. R., Norman, A., Quinn, P. K., Bates, T. S., Levasseur, M., Barrie, L. A., and Maenhaut, W.: Influence of transport and ocean ice extent on biogenic aerosol sulfur in the Arctic atmosphere, J. Geophys. Res.-Atmos., 117, D12209, doi:10.1029/2011JD017074, 2012. 1189

Snoeckx, H., Grousset, F., Revel, M., and Boelaert, A.: European contribution of ice-rafted sand to Heinrich layers H3 and H4, Mar. Geol., 158, 197–208, doi:10.1016/S0025-3227(98)00168-6, 1999. 1182

Sowers, T.: Late quaternary atmospheric CH_4 isotope record suggests marine clathrates are stable, Science, 311, 838–840, doi:10.1126/science.1121235, 2006. 1190

Stanford, J., Rohling, E., Bacon, S., Roberts, A., Grousset, F., and Bolshawa, M.: A new concept for the paleoceanographic evolution of Heinrich event 1 in the North Atlantic, Quaternary Sci. Rev., 30, 1047–1066, doi:10.1016/j.quascirev.2011.02.003, 2011. 1182

Stern, J. V. and Lisiecki, L. E.: North Atlantic circulation and reservoir age changes over the past 41,000 years, Geophys. Res. Lett., 40, 1–5, doi:10.1002/grl.50679, 2013. 1183

Stocker, T. F. and Johnsen, S. J.: A minimum thermodynamic model for the bipolar seesaw, Paleoceanography, 18, 1087, doi:10.1029/2003PA000920, 2003. 1181

Svensson, A., Andersen, K. K., Bigler, M., Clausen, H. B., Dahl-Jensen, D., Davies, S. M., Johnsen, S. J., Muscheler, R., Parrenin, F., Rasmussen, S. O., Röthlisberger, R., Seierstad, I., Steffensen, J. P., and Vinther, B. M.: A 60 000 year Greenland stratigraphic ice core chronology, Clim. Past, 4, 47–57, doi:10.5194/cp-4-47-2008, 2008. 1184, 1198

Toggweiler, J., Russell, J., and Carson, S.: Midlatitude westerlies, atmospheric CO_2, and climate change during the ice ages, Paleoceanography, 21, PA2005, doi:10.1029/2005PA001154, 2006. 1190

Vautravers, M. J., Shackleton, N. J., Lopez-Martinez, C., and Grimalt, J. O.: Gulf Stream variability during marine isotope stage 3, Paleoceanography, 19, PA2011, doi:10.1029/2003PA000966, 2004. 1192

Heinrich event 4 in Greenland ice core records

M. Guillevic et al.

Title Page

Abstract | Introduction

Conclusions | References

Tables | Figures

|◄ | ►|

◄ | ►

Back | Close

Full Screen / Esc

Printer-friendly Version

Interactive Discussion

Veres, D., Bazin, L., Landais, A., Toyé Mahamadou Kele, H., Lemieux-Dudon, B., Parrenin, F., Martinerie, P., Blayo, E., Blunier, T., Capron, E., Chappellaz, J., Rasmussen, S. O., Severi, M., Svensson, A., Vinther, B., and Wolff, E. W.: The Antarctic ice core chronology (AICC2012): an optimized multi-parameter and multi-site dating approach for the last 120 thousand years, Clim. Past, 9, 1733–1748, doi:10.5194/cp-9-1733-2013, 2013. 1214, 1220

Vinther, B. M., Clausen, H. B., Johnsen, S. J., Rasmussen, S. O., Andersen, K. K., Buchardt, S. L., Dahl-Jensen, D., Seierstad, I. K., Siggaard-Andersen, M.-L., Steffensen, J. P., and Svensson, A.: A synchronized dating of three Greenland ice cores throughout the Holocene, J. Geophys. Res., 111, D13102, doi:10.1029/2005JD006921, 2006. 1197

Voelker, A. H. L.: Global distribution of centennial-scale records for Marine Isotope Stage (MIS) 3: a database, Quaternary Sci. Rev., 21, 1185–1212, doi:10.1016/S0277-3791(01)00139-1, 2002. 1181

Völker, C. and Köhler, P.: Responses of ocean circulation and carbon cycle to changes in the position of the Southern Hemisphere westerlies at Last Glacial Maximum, Paleoceanography, 28, 726–739, doi:10.1002/2013PA002556, 2013. 1190

Waelbroeck, C., Duplessy, J.-C., Michel, E., Labeyrie, L., Paillard, D., and Duprat, J.: The timing of the last deglaciation in North Atlantic climate records, Nature, 412, 724–727, doi:10.1038/35089060, 2001. 1183

Wang, X., Auler, A. S., Edwards, R. L., Cheng, H., Ito, E., Wang, Y., Kong, X., and Solheid, M.: Millennial-scale precipitation changes in southern Brazil over the past 90,000 years, Geophys. Res. Lett., 34, L23701, doi:10.1029/2007GL031149, 2007. 1183

Wang, Y. J., Cheng, H., Edwards, R. L., An, Z. S., Wu, J. Y., Shen, C. C., and Dorale, J. A.: A high-resolution absolute-dated Late Pleistocene monsoon record from Hulu Cave, China, Science, 294, 2345–2348, doi:10.1126/science.1064618, 2001. 1181, 1183

Wolff, E. W., Chappellaz, J., Blunier, T., Rasmussen, S. O., and Svensson, A.: Millennial-scale variability during the last glacial: the ice core record, Quaternary Sci. Rev., 29, 2828–2838, doi:10.1016/j.quascirev.2009.10.013, 2010. 1198

Zumaque, J., Eynaud, F., Zaragosi, S., Marret, F., Matsuzaki, K. M., Kissel, C., Roche, D. M., Malaizé, B., Michel, E., Billy, I., Richter, T., and Palis, E.: An ocean–ice coupled response during the last glacial: a view from a marine isotopic stage 3 record south of the Faeroe Shetland Gateway, Clim. Past, 8, 1997–2017, doi:10.5194/cp-8-1997-2012, 2012. 1196

Discussion Paper | Discussion Paper | Discussion Paper | Discussion Paper |

Table 1. Timing and duration of the climatic fingerprints associated with Heinrich events 4 and 5 on the GICC05 timescale. Column 2: onsets of GI and GS are given according to Rasmussen et al. (2014). Column 3: maximum counting error (MCE), reflecting the number of uncertain annual layers compared to year AD 2000 (Rasmussen et al., 2006, and Appendix A1). Column 5: MCE of the phase duration, calculated as the MCE difference between start and end of each phase. Column 6: total duration uncertainty for each phase: MCE of the phase duration, synchronisation uncertainty of the NEEM ice core to the NGRIP GICC05 timescale (~ 20 a, Rasmussen et al., 2013) and data resolution (± 35 a in average).

	start time		duration		
	a b2k	MCE, a	a	MCE, a	total uncertainty (2σ), a
GS-13					
Phase 1	48 340	1988	140	7	40
Phase 2	48 200	1981	860	43	60
Phase 3	47 340	1938	480	26	50
GI-12	46 860	1912			
GS-9					
Phase 1	39 900	1569	550	51	60
Phase 2	39 350	1518	740	47	60
Phase 3	38 610	1471	390	22	50
GI-8	38 220	1449			

Table 2. Match points between methane depths from the Byrd ice core (Ahn and Brook, 2008; Ahn et al., 2012), the Siple Dome ice core (Brook et al., 2005; Ahn et al., 2012) and NEEM methane (Chappellaz et al., 2013) gas age according to the GICC05 chronology (Guillevic et al., 2013; Rasmussen et al., 2013).

Event	Byrd depth, m	Siple Dome depth, m	NEEM methane gas age, a b2k
GI-6	1617.15	795.37	33 716
GI-7	1654.05	809.97	35 435
GI-8, dip	1691.10	818.13	36 901
GI-8	1716.10	825.66	38 125
GS-9, methane plateau	1743.55	833.81	39 372
GI-9	1759.20	837.90	40 121
GI-10	1780.30	845.97	41 467
GI-11	1807.95	855.28	43 351
GI-12	1863.05		46 859
GI-13	1898.30		49 276
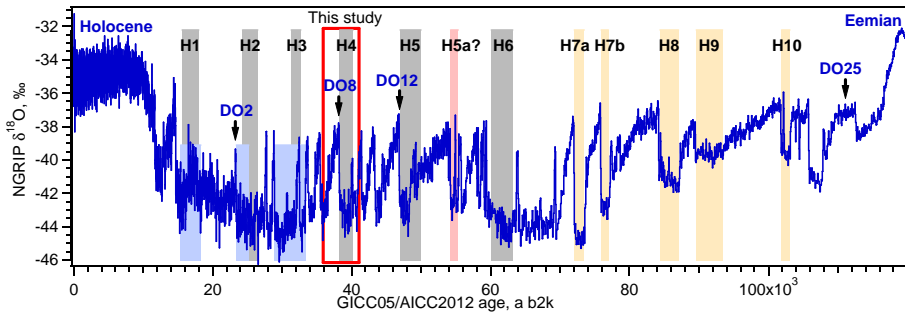
Fig. 1. Dansgaard–Oeschger (DO) and Heinrich (H) events during the last glacial period. Blue line: NGRIP δ^{18}O, ‰ (NGRIP members, 2004), on the GICC05 timescale back to 60 ka b2k (Appendix A1) and AICC2012 beyond (Bazin et al., 2013; Veres et al., 2013). Grey areas: position and duration of H1 to H6, major Heinrich events recorded in marine cores from the North Atlantic (Sánchez Goñi and Harrison, 2010). Blue areas: periods of low salinity corresponding to fresh water input on the Celtic Margin (Eynaud et al., 2012). H5a (pink) and H7 to H10 (yellow) are minor IRD events, recorded in the West Atlantic (Rashid et al., 2003; Rasmussen et al., 2003).

Heinrich event 4 in Greenland ice core records

M. Guillevic et al.
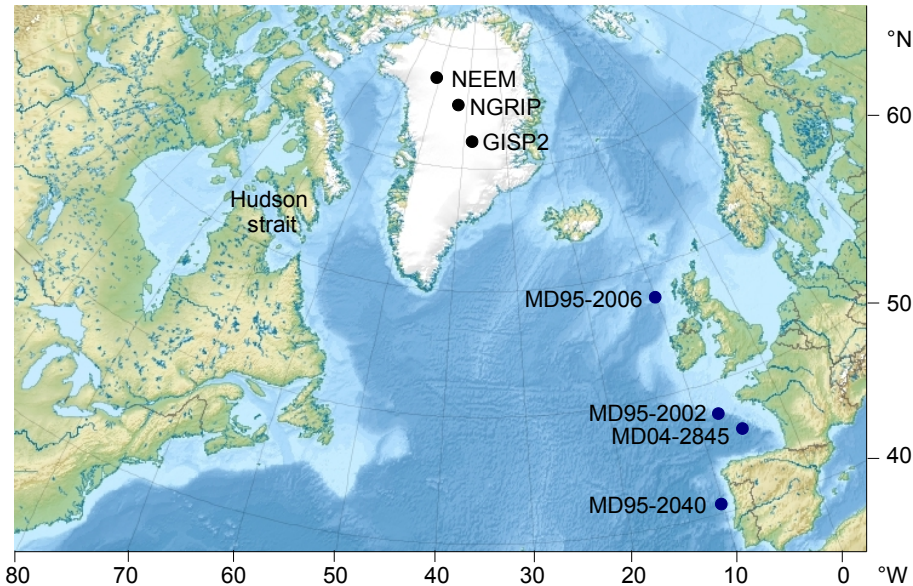
Fig. 2. Map of the Northern Hemisphere palaeoclimate archives used in this study. Blue dots: marine cores. Black dots: ice cores. Most of the IRD for H4 and H5 were deposited by icebergs originating from the Laurentide ice sheet and delivered through Hudson Strait (Hemming, 2004). All marine cores on the map contain Laurentide IRD for H4 and H5. Background map from Uwe Dedering.
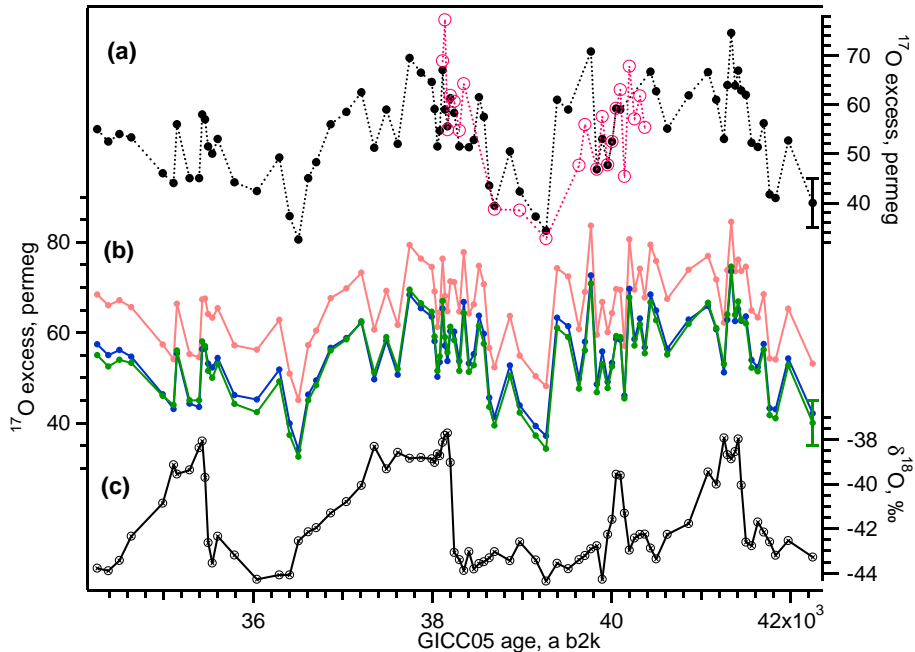
Fig. 3. NEEM ^{17}O excess (permeg) and δ^{18}O (‰) data. **(a)** Comparison of the ^{17}O excess data measured in spring 2011 (black dots) and at the beginning of 2012 (pink circles). **(b)** Calibration of the ^{17}O excess data. Pink dots: measured data; blue dots: one point calibration; green dots: two points calibration. **(c)** δ^{18}O, ‰.
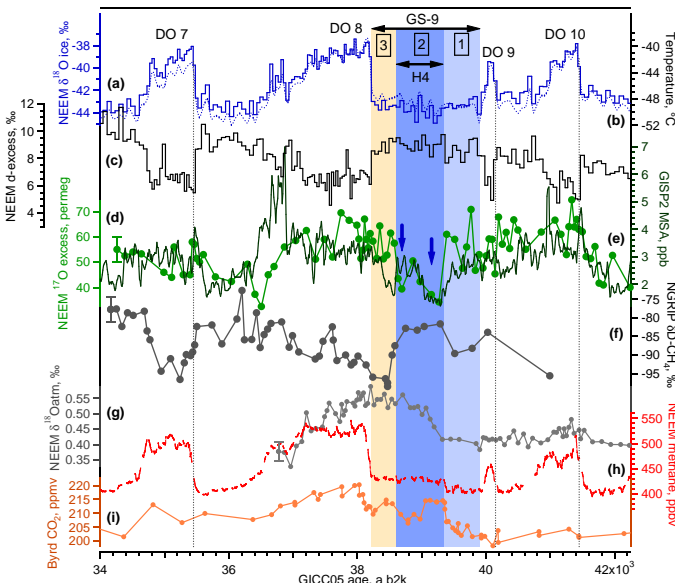
Fig. 4. Greenland and Antarctic ice core records surrounding Heinrich event 4, synchronised to the GICC05 timescale (Appendix A). Position of phase 1 (light blue area), phase 2 (blue area) and phase 3 (yellow area) as given in Table 1. The blue arrows indicate two potential iceberg pulses. **(a)** Blue line: NEEM δ^{18}O ice, ‰ (precision: 0.07‰) (Guillevic et al., 2013). **(b)** Blue dotted line: NEEM temperature reconstructed using δ^{15}N data and firn modeling (Guillevic et al., 2013). **(c)** Black: NEEM deuterium excess, ‰ (±0.7‰), this study, measured at LSCE (France). **(d)** Green dots: NEEM ^{17}O excess, permeg (±5 permeg), this study, measured at LSCE. Each dot corresponds to the average over 55 cm of ice. **(e)** Dark green: GISP2 MSA concentration data (Saltzman et al., 1997), ppb, 50 a running average. **(f)** Dark grey: NGRIP δD-CH$_4$, ‰ (±3.4‰) (Bock et al., 2010). **(g)** Light grey: NEEM δ^{18}O$_{atm}$, ‰ (±0.03‰), this study, measured at LSCE. **(h)** Red: NEEM methane mixing ratio, ppbv (±5 ppbv), record measured by the Picarro instrument (Chappellaz et al., 2013). **(i)** Orange: CO$_2$ mixing ratio, ppmv (±1 ppmv), from the Byrd ice core, Antarctica (Ahn et al., 2012).

Discussion Paper | Discussion Paper | Discussion Paper | Discussion Paper

Title Page

Abstract | Introduction

Conclusions | References

Tables | Figures

|◄ | ►|

◄ | ►

Back | Close

Full Screen / Esc

Printer-friendly Version

Interactive Discussion
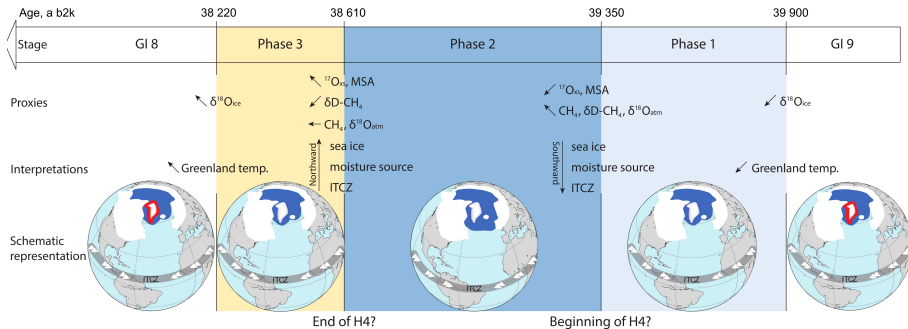
Fig. 5. Sequence of events indicated by the proxy records and our climatic interpretation. The globes give a schematic representation of the sea ice extent (in dark blue), the position of the ITCZ, and Greenland temperature (red representing warm conditions).
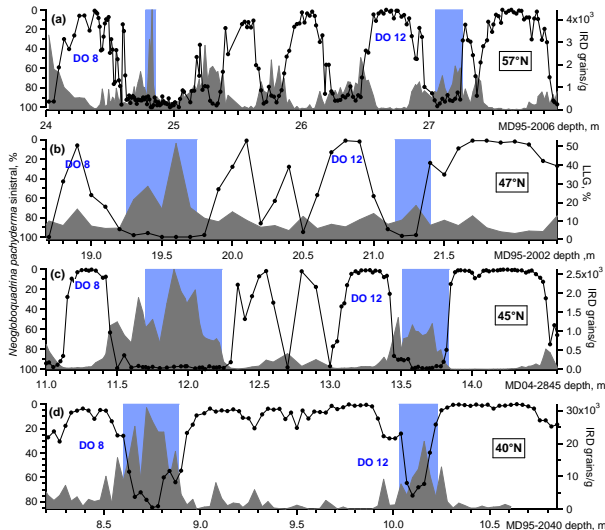
Fig. 6. H4 and H5 in marine core records from the European margin. Core localisations are shown in Fig. 2. Note that each core is on its own depth scale, there is no synchronisation in-between cores. **(a)** Core MD95-2006, Barra Fan, 57° 01′82 N, 10° 03′48 W (Peters et al., 2008; Dickson et al., 2008). **(b)** Core MD95-2002, Celtic margin, 47° 27′12 N, 8° 27′03 W (Auffret et al., 2002). **(c)** Core MD04-2845, Bay of Biscay, 45° 21′ N, 5° 13′ W (Sánchez-Goñi et al., 2008). **(d)** Core MD95-2040, Portugese margin, 40° 34′91 N, 9° 51′67 W (de Abreu et al., 2003; Eynaud et al., 2009). Grey shaded area: IRD or LLG (large lithic grains), counted on the $> 150\,\mu$m fraction. Black line and dots: abundance of the polar foraminifer *N. pachyderma* sinistral, %; a high percentage denotes cold sea surface temperature. Blue shaded areas: IRD/LGG from the Laurentide ice sheet. Origin identification of IRD for core MD95-2006 based on mineral magnetic measurements (for H4 and H5, Peters et al., 2008) and an additional unpublished count of detrital carbonate grains (for H4, W. Austin, personal communication, 2014), on ε neodym and magnetic susceptibility for core MD95-2002 (Auffret et al., 2002) and on magnetic susceptibility for core MD04-2845 (Sánchez-Goñi et al., 2008) and MD95-2040 (de Abreu et al., 2003).

Heinrich event 4 in Greenland ice core records

M. Guillevic et al.

Title Page

Abstract · Introduction

Conclusions · References

Tables · Figures

|◄ · ►|

◄ · ►

Back · Close

Full Screen / Esc

Printer-friendly Version

Interactive Discussion
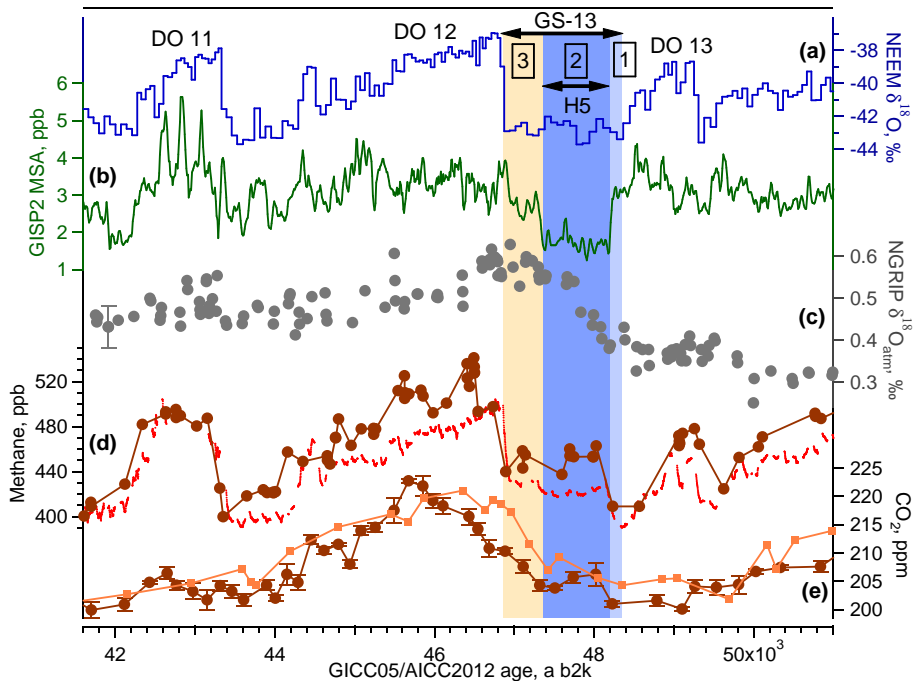
Fig. 7. Sequence of events for Heinrich event 5 in multi-proxy ice core records. Position of phase 1 (light blue area), phase 2 (blue area) and phase 3 (yellow area) as given in Table 1. **(a)** NEEM $\delta^{18}O$, ‰, this study. **(b)** GISP2 MSA concentration data, ppb (Saltzman et al., 1997), 50 a running average. **(c)** NGRIP $\delta^{18}O_{atm}$, ‰ (Huber et al., 2006). **(d)** Red line: NEEM methane mixing ratio (Chappellaz et al., 2013, we use here the record measured by the Picarro instrument). Brown dots: TALDICE methane record (Buiron et al., 2011). **(e)** Brown: TALDICE CO_2, ppm (Bereiter et al., 2012). Orange: Byrd CO_2, ppm (Ahn et al., 2012). Data from the TALDICE ice core are displayed on the AICC2012 timescale (Veres et al., 2013; Bazin et al., 2013) and all other datasets on the GICC05 timescale (see Appendix A). Note than both timescales are compatible during the presented time period.

Title Page

Abstract | Introduction

Conclusions | References

Tables | Figures

|◄ | ►|

◄ | ►

Back | Close

Full Screen / Esc

Printer-friendly Version

Interactive Discussion
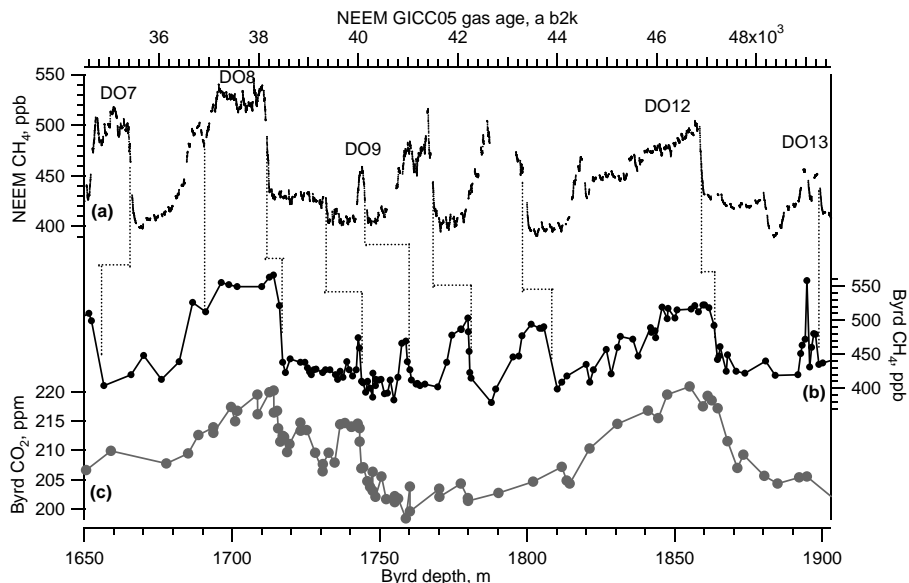
Fig. 8. Construction of a gas age scale for the Byrd ice core. **(a)** NEEM methane data (Chappellaz et al., 2013) on the NEEM GICC05 gas age scale (Guillevic et al., 2013). **(b)** CH_4 and **(c)** CO_2 data from the Byrd ice core on a depth scale (Ahn et al., 2012). The dotted black lines indicate the match points (Table 2) used to tie the Byrd record to the NEEM GICC05 gas age scale.
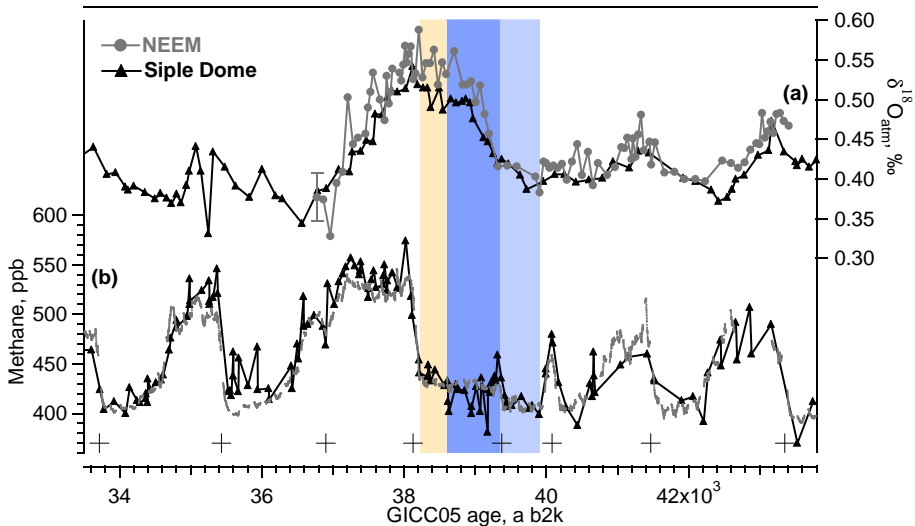
Fig. 9. Comparison of Siple Dome and NEEM $\delta^{18}O_{atm}$ records. **(a)** NEEM (grey dots, this study) and Siple Dome (black triangles, Severinghaus et al., 2009) $\delta^{18}O_{atm}$ data on the GICC05 timescale. **(b)** NEEM (grey line, Chappellaz et al., 2013) and Siple Dome (black triangles, Brook et al., 2005; Ahn et al., 2012) methane data on the GICC05 timescale (Guillevic et al., 2013). The Siple Dome methane record is matched to the NEEM methane record using the match points (Table 2) indicated by the black crosses. Light blue, blue and yellow areas: phases 1, 2 and 3 of GS-9, respectively.

Title Page

Abstract | Introduction

Conclusions | References

Tables | Figures

|◄ | ►|

◄ | ►

Back | Close

Full Screen / Esc

Printer-friendly Version

Interactive Discussion